Density Model for Killer Whale (*Orcinus orca*) for the U.S. Gulf of Mexico: Supplementary Report

Duke University Marine Geospatial Ecology Lab*

Model Version 1.3 - 2015-09-30

Citation

When referencing our methodology or results generally, please cite our open-access article:

Roberts JJ, Best BD, Mannocci L, Fujioka E, Halpin PN, Palka DL, Garrison LP, Mullin KD, Cole TVN, Khan CB, McLellan WM, Pabst DA, Lockhart GG (2016) Habitat-based cetacean density models for the U.S. Atlantic and Gulf of Mexico. Scientific Reports 6: 22615. doi: 10.1038/srep22615

To reference this specific model or Supplementary Report, please cite:

Roberts JJ, Best BD, Mannocci L, Fujioka E, Halpin PN, Palka DL, Garrison LP, Mullin KD, Cole TVN, Khan CB, McLellan WM, Pabst DA, Lockhart GG (2015) Density Model for Killer Whale (*Orcinus orca*) for the U.S. Gulf of Mexico Version 1.3, 2015-09-30, and Supplementary Report. Marine Geospatial Ecology Lab, Duke University, Durham, North Carolina.

Copyright and License

Revision History

Version	Date	Description of changes
1	2015-01-13	Initial version.
1.1	2015-02-02	Updated the documentation. No changes to the model.
1.2	2015-05-14	Updated calculation of CVs. Switched density rasters to logarithmic breaks. No changes to the model.
1.3	2015-09-30	Updated the documentation. No changes to the model.

*For questions, or to offer feedback about this model or report, please contact Jason Roberts (jason.roberts@duke.edu)

Survey Data

Survey	Period	Length (1000 km)	Hours	Sightings
SEFSC GOMEX92-96 Aerial Surveys	1992-1996	27	152	0
SEFSC Gulf of Mexico Shipboard Surveys, 2003-2009	2003-2009	19	1156	3
SEFSC GulfCet I Aerial Surveys	1992-1994	50	257	0
SEFSC GulfCet II Aerial Surveys	1996-1998	22	124	0
SEFSC GulfSCAT 2007 Aerial Surveys	2007-2007	18	95	0
SEFSC Oceanic CetShip Surveys	1992-2001	49	3102	13
SEFSC Shelf CetShip Surveys	1994-2001	10	707	0
Total		195	5593	16

Table 2: Survey effort and sightings used in this model. Effort is tallied as the cumulative length of on-effort transects and hours the survey team was on effort. Sightings are the number of on-effort encounters of the modeled species for which a perpendicular sighting distance (PSD) was available. Off effort sightings and those without PSDs were omitted from the analysis.

Period	Length (1000 km)	Hours	Sightings
1992-2009	195	5592	16
1998-2009	62	2679	7
% Lost	68	52	56

Table 3: Survey effort and on-effort sightings having perpendicular sighting distances. % Lost shows the percentage of effort or sightings lost by restricting the analysis to surveys performed in 1998 and later, the era in which remotely-sensed chlorophyll and derived productivity estimates are available. See Figure 1 for more information.

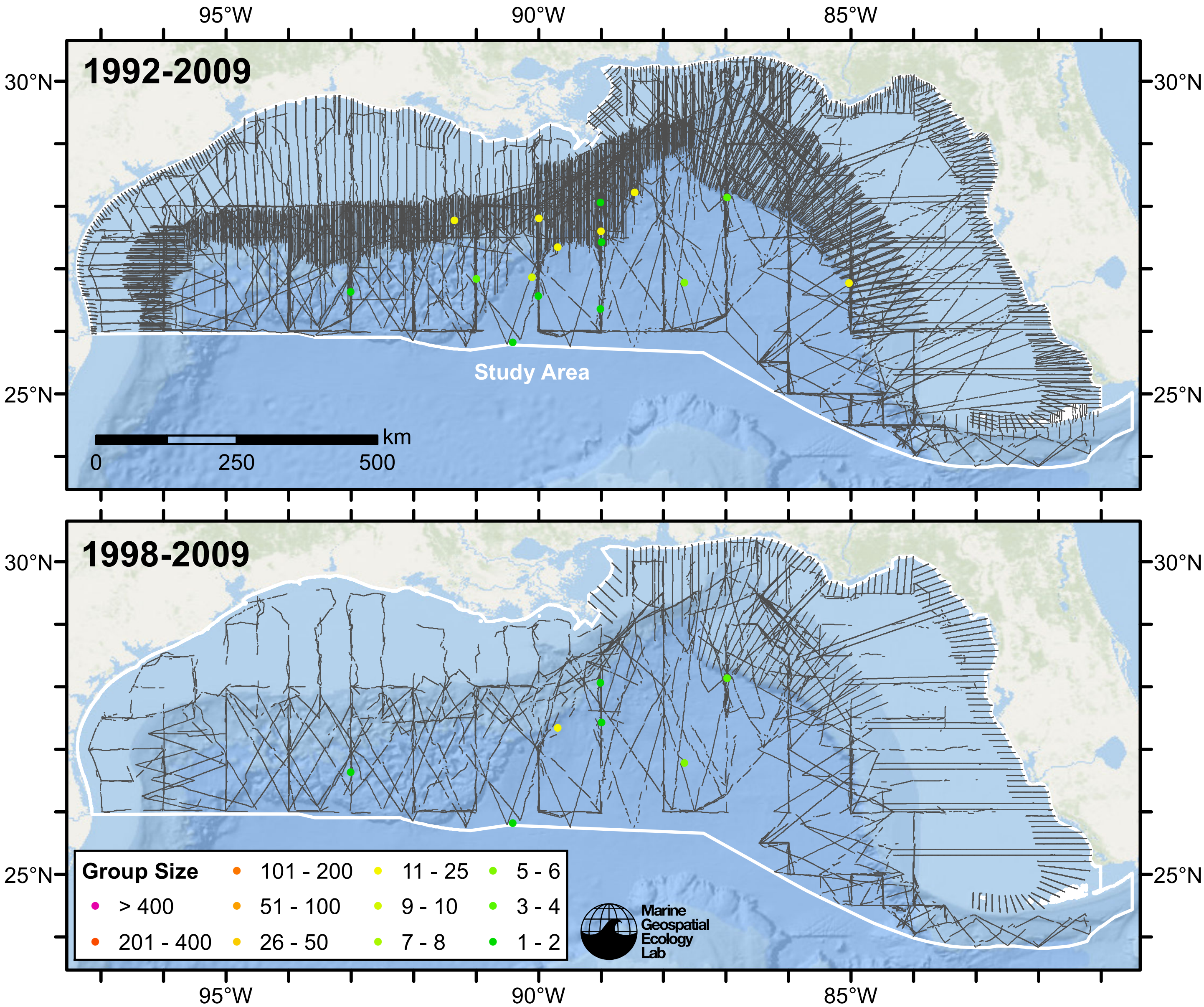

Figure 1: Killer whale sightings and survey tracklines. The top map shows all surveys. The bottom map shows surveys performed in 1998 or later. the era in which remotely-sensed chlorophyll and derived productivity estimates are available. Models fitted to contemporaneous (day-of-sighting) estimates of those predictors only utilize these surveys. These maps illustrate the survey data lost in order to utilize those predictors. Models fitted to climatogical estimates of those predictors do not suffer this data loss.

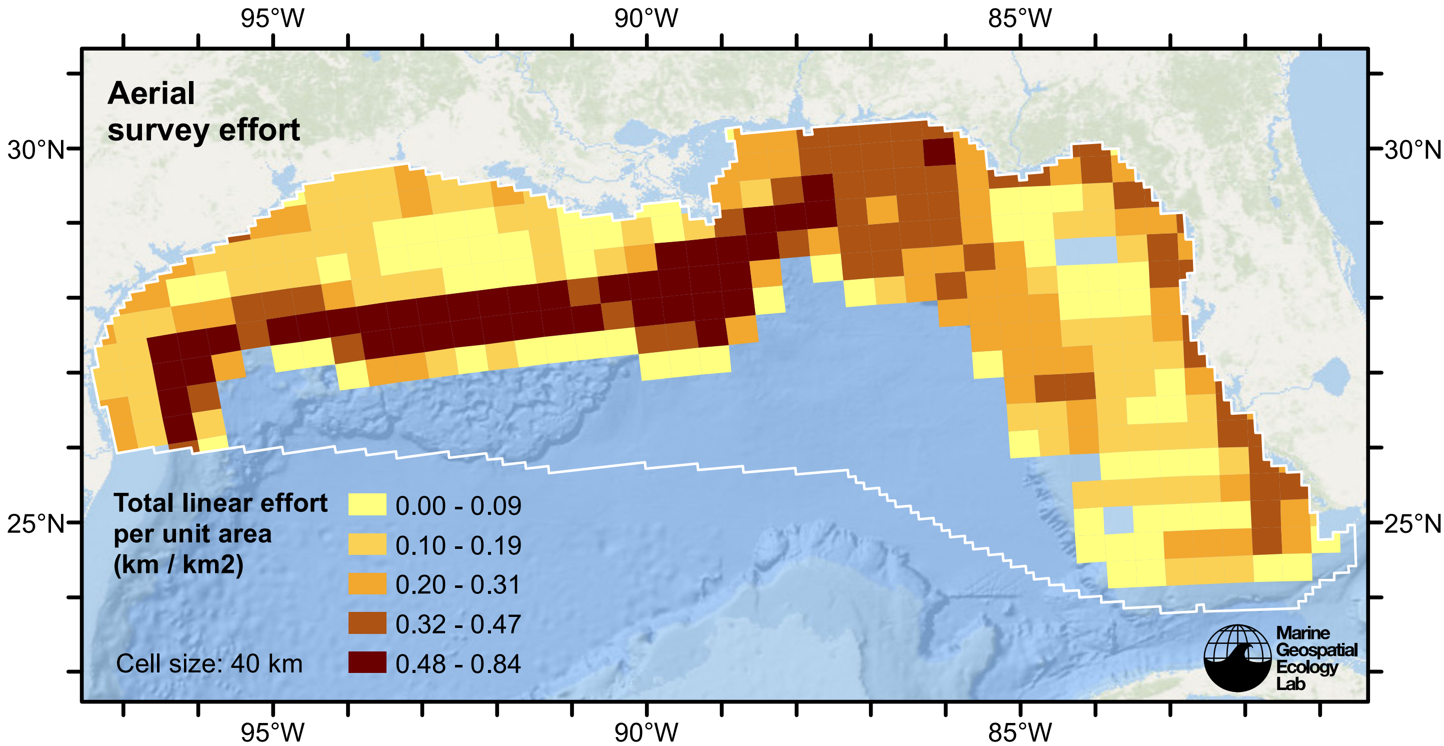

Figure 2: Aerial linear survey effort per unit area.

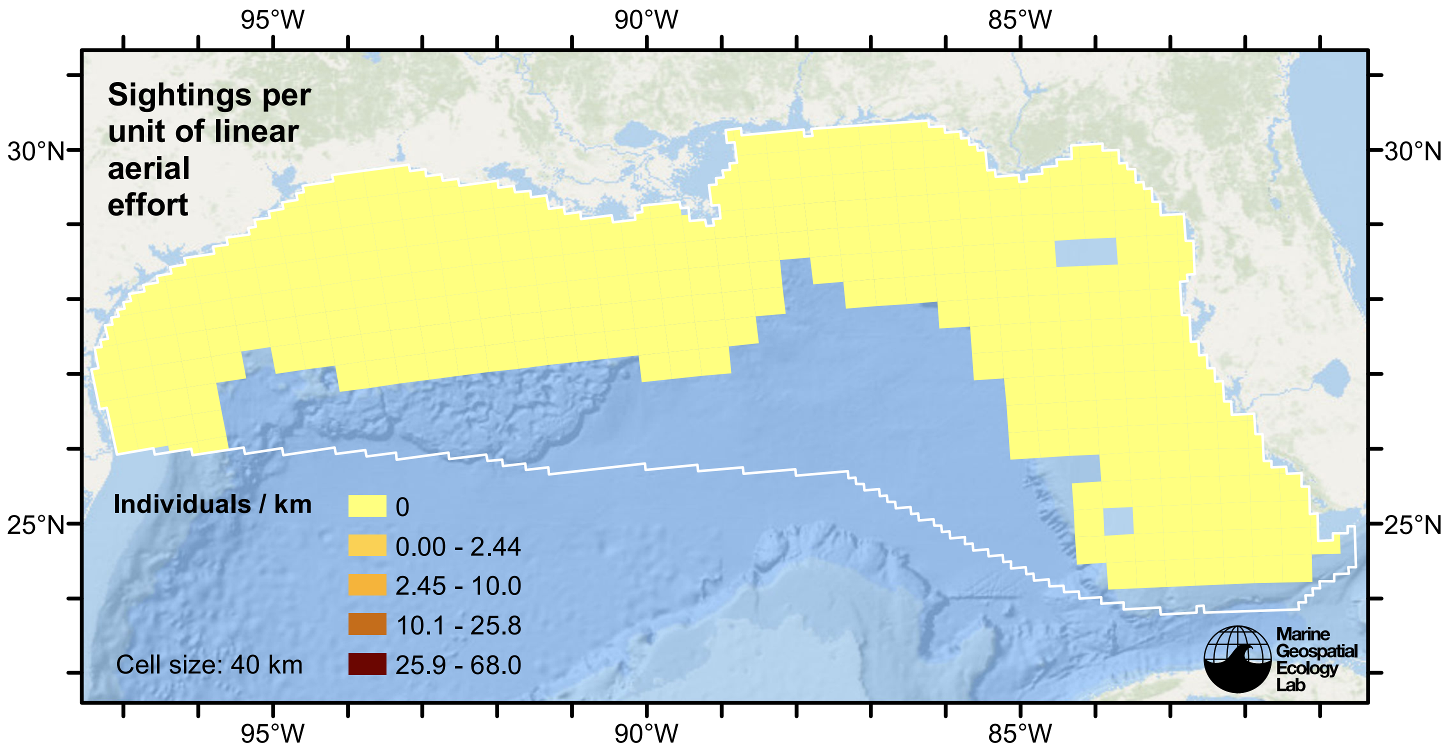

Figure 3: Killer whale sightings per unit aerial linear survey effort.

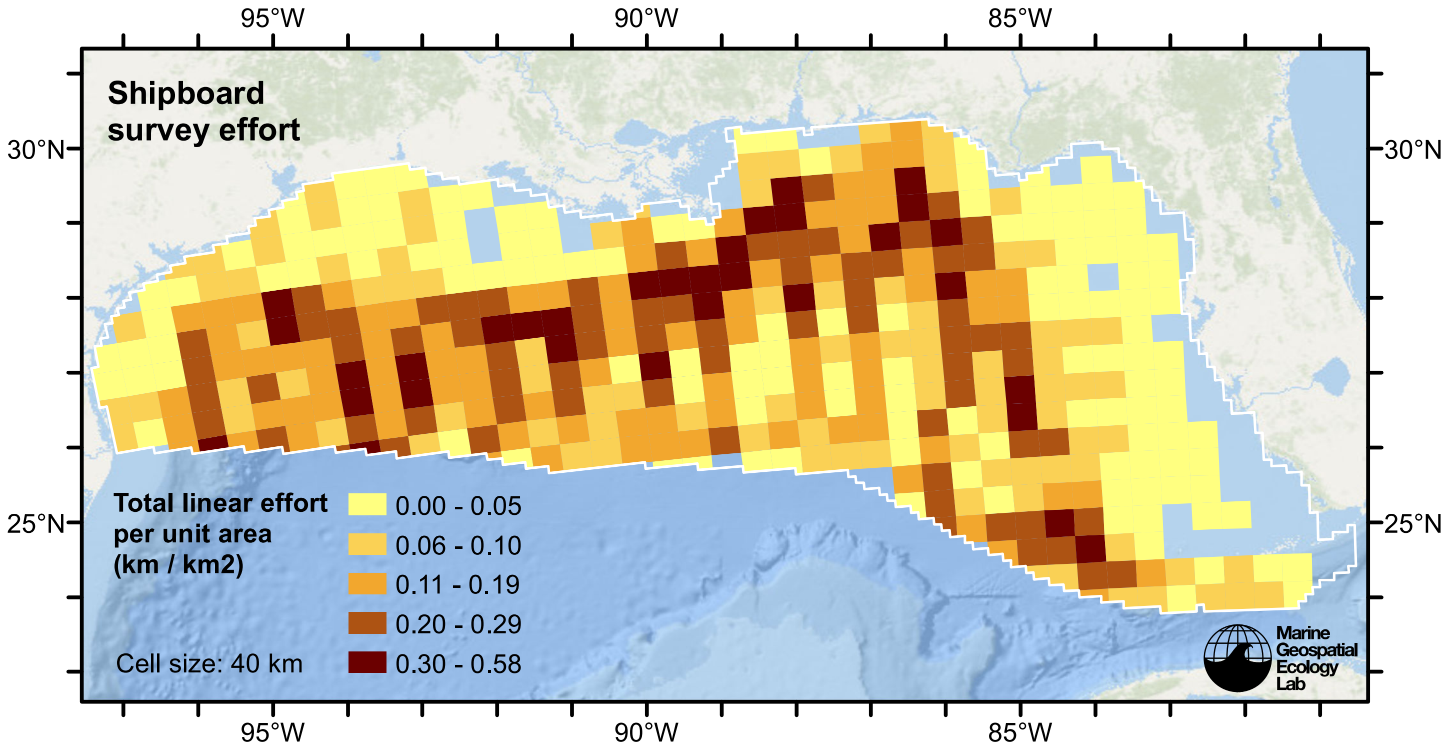

Figure 4: Shipboard linear survey effort per unit area.

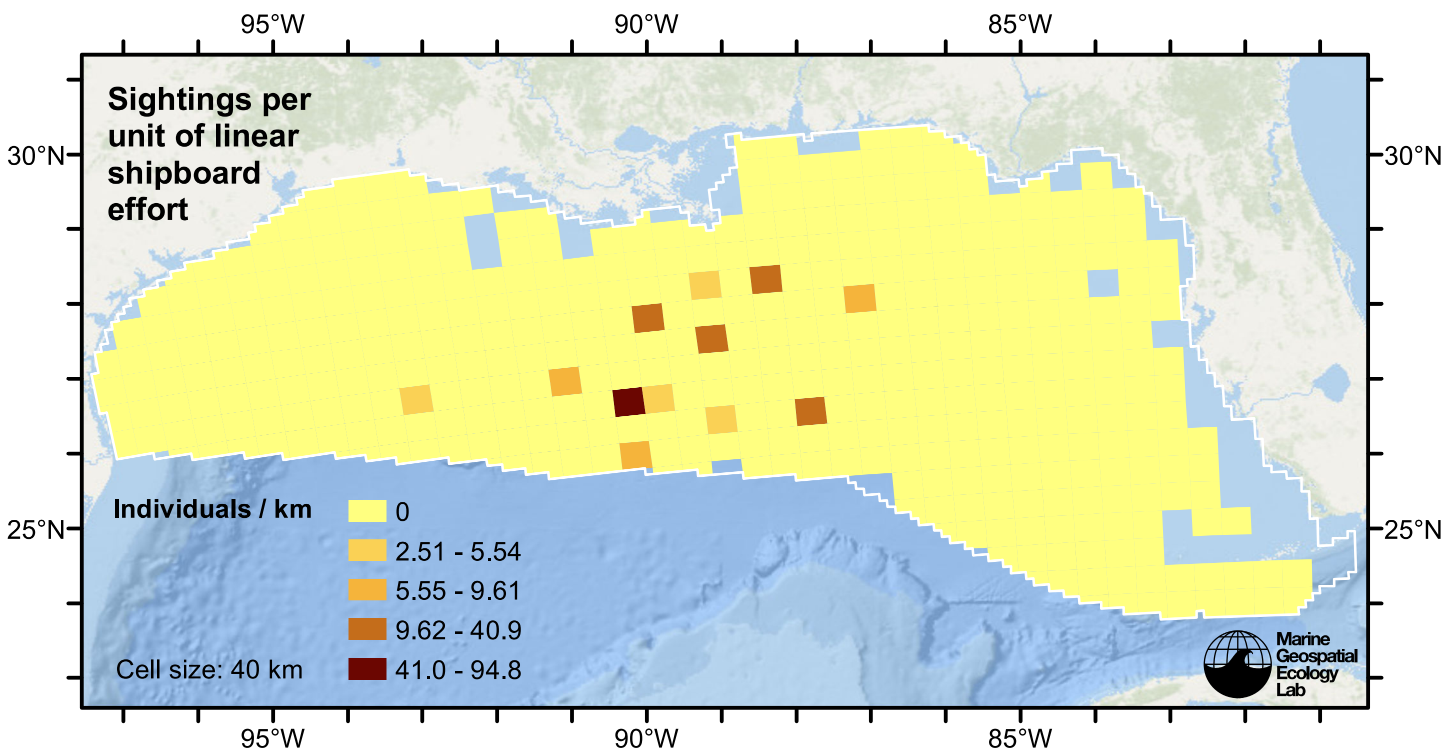

Figure 5: Killer whale sightings per unit shipboard linear survey effort.

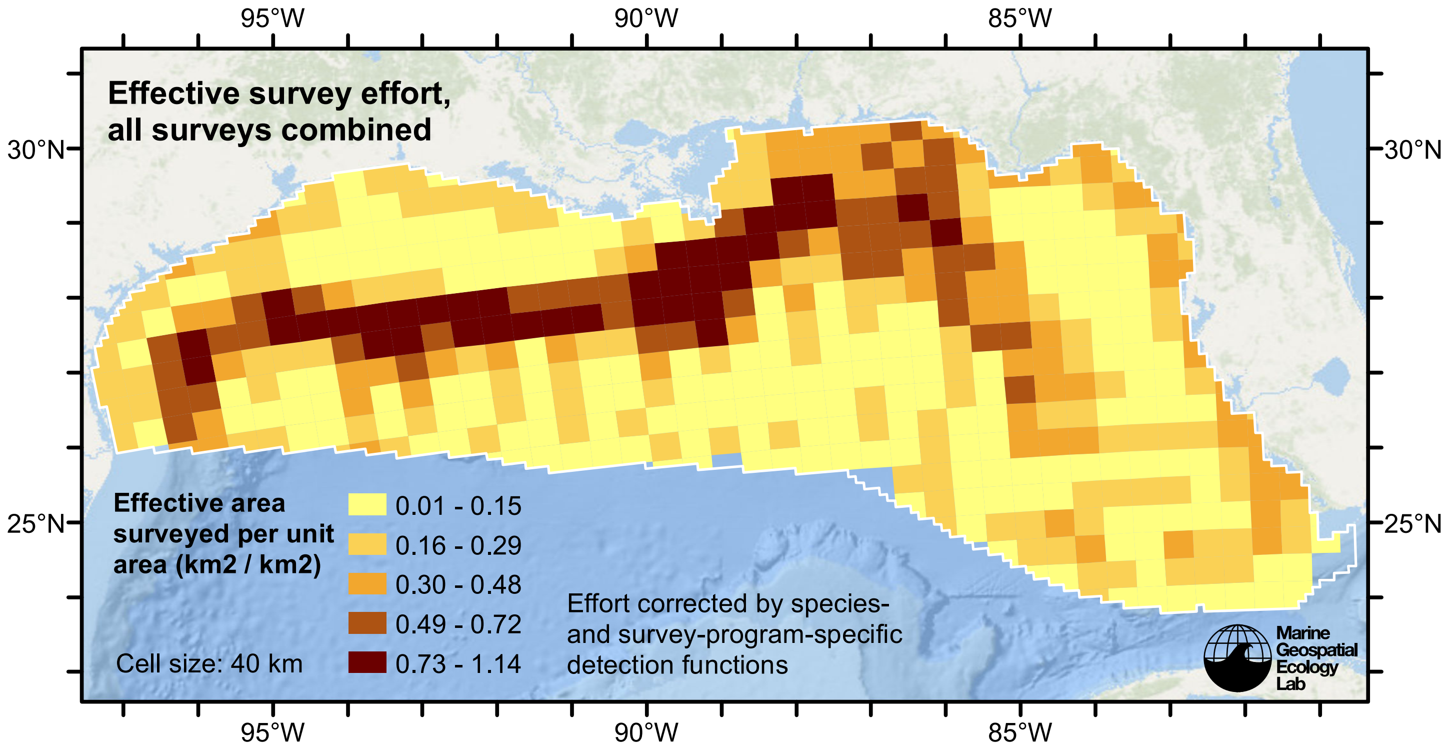

Figure 6: Effective survey effort per unit area, for all surveys combined. Here, effort is corrected by the species- and survey-program-specific detection functions used in fitting the density models.

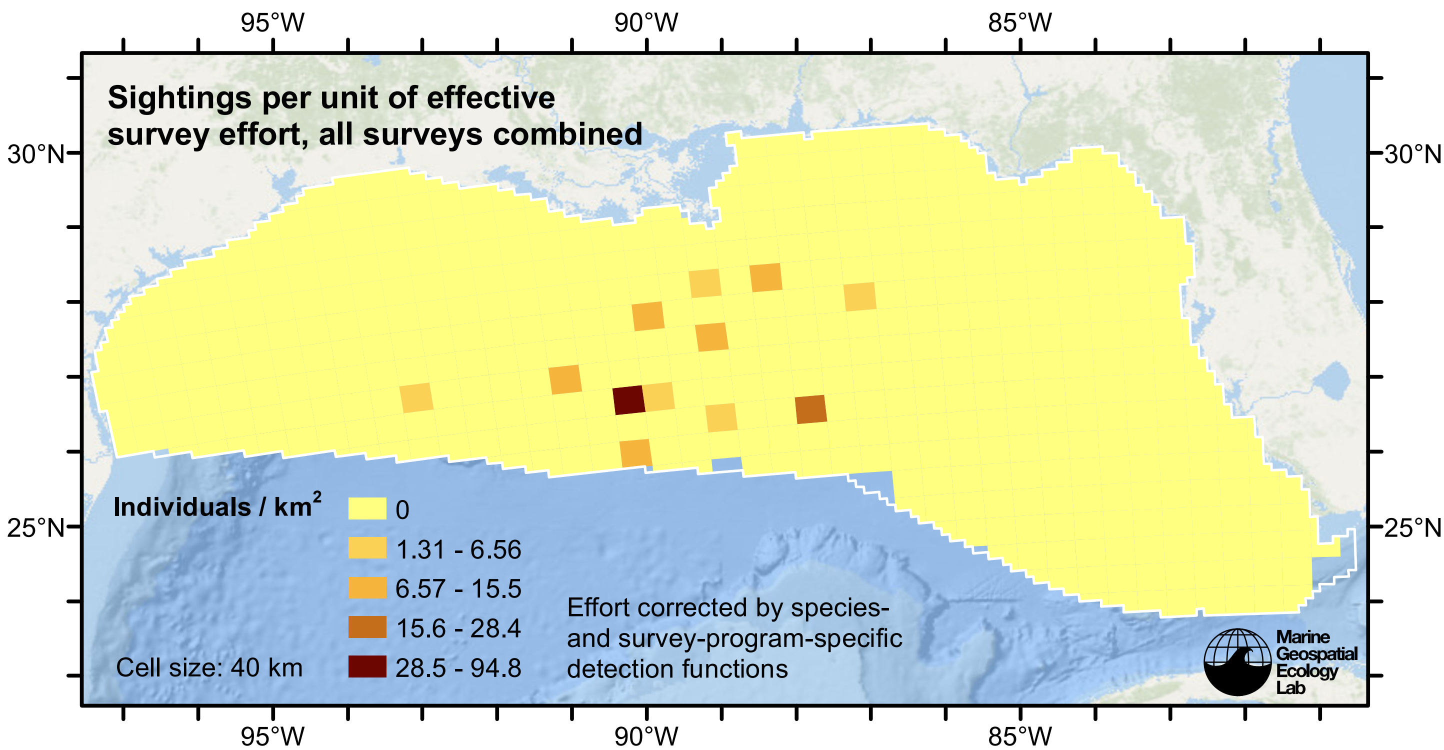

Figure 7: Killer whale sightings per unit of effective survey effort, for all surveys combined. Here, effort is corrected by the species- and survey-program-specific detection functions used in fitting the density models.

Detection Functions

The detection hierarchy figures below show how sightings from multiple surveys were pooled to try to achieve Buckland et. al's (2001) recommendation that at least 60-80 sightings be used to fit a detection function. Leaf nodes, on the right, usually represent individual surveys, while the hierarchy to the left shows how they have been grouped according to how similar we believed the surveys were to each other in their detection performance.

At each node, the red or green number indicates the total number of sightings below that node in the hierarchy, and is colored green if 70 or more sightings were available, and red otherwise. If a grouping node has zero sightings–i.e. all of the surveys within it had zero sightings–it may be collapsed and shown as a leaf to save space.

Each histogram in the figure indicates a node where a detection function was fitted. The actual detection functions do not appear in this figure; they are presented in subsequent sections. The histogram shows the frequency of sightings by perpendicular sighting distance for all surveys contained by that node. Each survey (leaf node) recieves the detection function that is closest to it up the hierarchy. Thus, for common species, sufficient sightings may be available to fit detection functions deep in the hierarchy, with each function applying to only a few surveys, thereby allowing variability in detection performance between surveys to be addressed relatively finely. For rare species, so few sightings may be available that we have to pool many surveys together to try to meet Buckland's recommendation, and fit only a few coarse detection functions high in the hierarchy.

A blue Proxy Species tag indicates that so few sightings were available that, rather than ascend higher in the hierarchy to a point that we would pool grossly-incompatible surveys together, (e.g. shipboard surveys that used big-eye binoculars with those that used only naked eyes) we pooled sightings of similar species together instead. The list of species pooled is given in following sections.

Shipboard Surveys

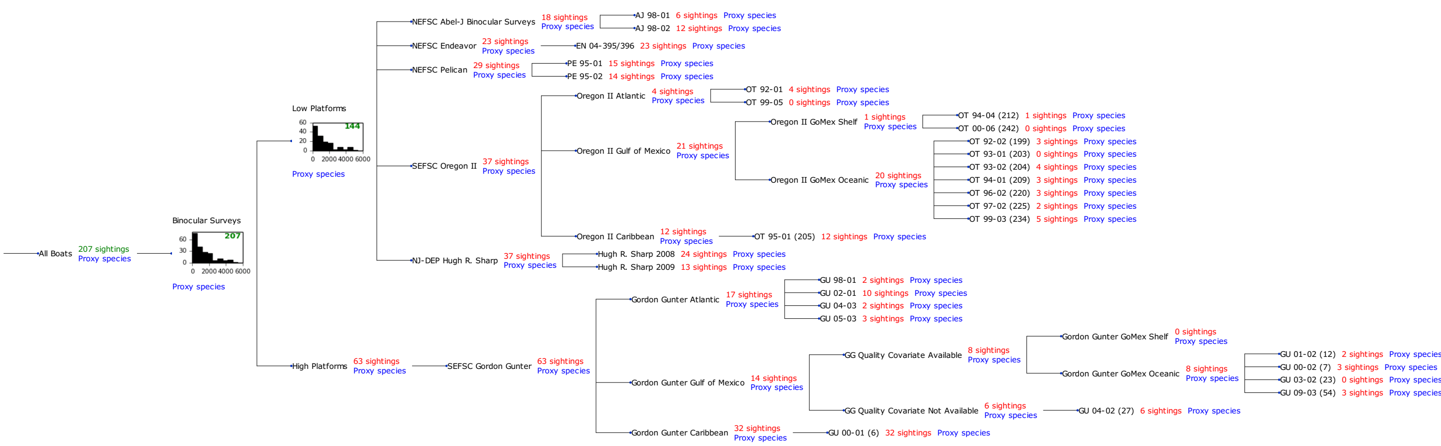

Figure 8: Detection hierarchy for shipboard surveys

Binocular Surveys

Because this taxon was sighted too infrequently to fit a detection function to its sightings alone, we fit a detection function to the pooled sightings of several other species that we believed would exhibit similar detectability. These "proxy species" are listed below.

Reported By Observer	Common Name	n
Balaenoptera	Balaenopterid sp.	8
Balaenoptera acutorostrata	Minke whale	4
Balaenoptera borealis	Sei whale	4
Balaenoptera borealis/edeni	Sei or Bryde's whale	6

Balaenoptera borealis/physalus	Fin or Sei whale	0
Balaenoptera edeni	Bryde's whale	21
Balaenoptera musculus	Blue whale	0
Balaenoptera physalus	Fin whale	98
Eubalaena glacialis	North Atlantic right whale	4
Eubalaena glacialis/Megaptera novaeangliae	Right or humpback whale	0
Megaptera novaeangliae	Humpback whale	46
Orcinus orca	Killer whale	16
Total		207

Table 4: Proxy species used to fit detection functions for Binocular Surveys. The number of sightings, n, is before truncation.

The sightings were right truncated at 5500m.

Covariate	Description
beaufort	Beaufort sea state.
size	Estimated size (number of individuals) of the sighted group.
vessel	Vessel from which the observation was made. This covariate allows the detection function to account for vessel-specific biases, such as the height of the survey platform.

Table 5: Covariates tested in candidate "multi-covariate distance sampling" (MCDS) detection functions.

Key	Adjustment	Order	Covariates	Succeeded	Δ AIC	Mean ESHW (m)
hr	poly	2		Yes	0.00	1242
hr	poly	4		Yes	0.30	1229
hr				Yes	1.55	1436
hr			beaufort	Yes	3.54	1439
hn	cos	2		Yes	3.91	1779
hr			vessel	Yes	6.82	1585
hr			beaufort, vessel	Yes	8.65	1612
hn	cos	3		Yes	11.95	1743
hn			vessel	Yes	19.94	2284
hn				Yes	22.38	2297
hn			beaufort	Yes	24.09	2296
hn			size	Yes	24.31	2391
hn			beaufort, size	Yes	26.18	2393
hn	herm	4		No		
hr			size	No		

hn	beaufort, vessel	No
hr	beaufort, size	No
hn	vessel, size	No
hr	vessel, size	No
hn	beaufort, vessel, size	No
hr	beaufort, vessel, size	No

Table 6: Candidate detection functions for Binocular Surveys. The first one listed was selected for the density model.

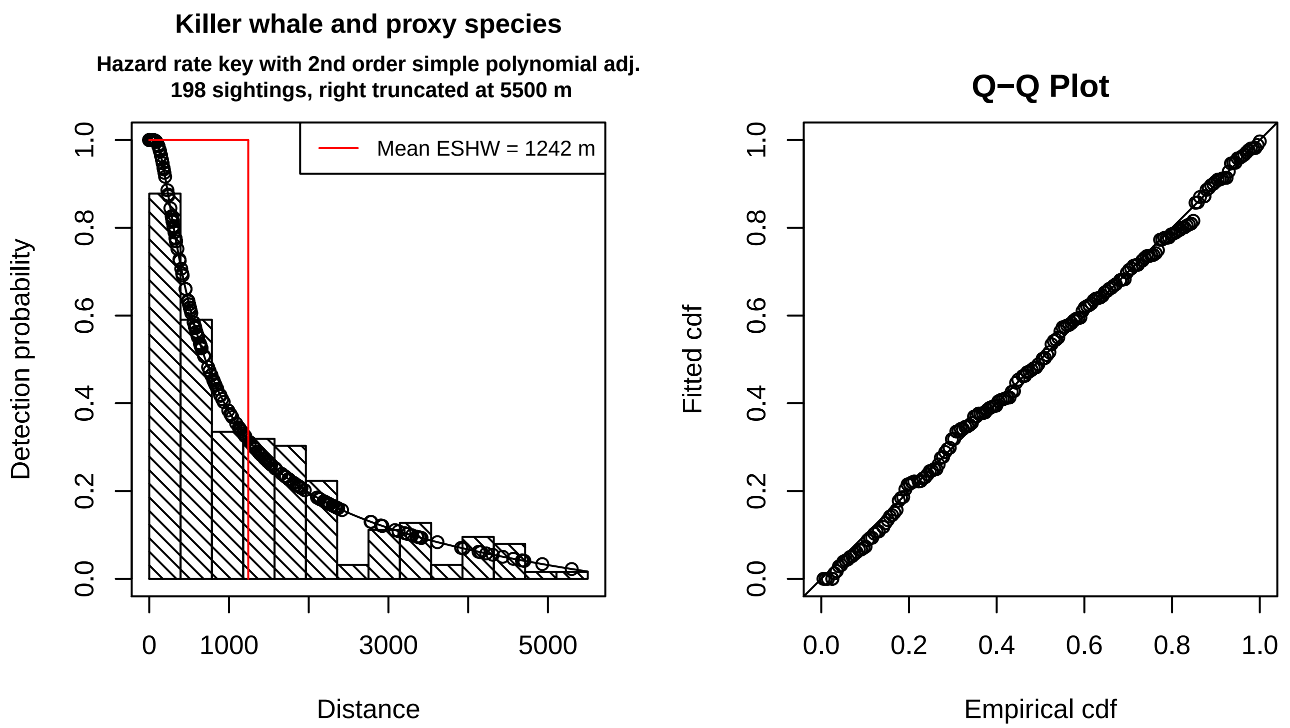

Figure 9: Detection function for Binocular Surveys that was selected for the density model

Statistical output for this detection function:

```
Summary for ds object
Number of observations :  198
Distance range         :  0  -  5500
AIC                    :  3236.988

Detection function:
 Hazard-rate key function with simple polynomial adjustment term of order 2

Detection function parameters
Scale Coefficients:
            estimate        se
(Intercept) 6.208036 0.3983515

Shape parameters:
```

```
                 estimate        se
(Intercept) 2.160139e-07 0.2156349

Adjustment term parameter(s):
                estimate       se
poly, order 2 -0.808364 0.237676


Monotonicity constraints were enforced.
                        Estimate           SE        CV
Average p              0.2257851   0.03930817 0.1740955
N in covered region 876.9400254 162.22067785 0.1849849

Monotonicity constraints were enforced.
```

Additional diagnostic plots:

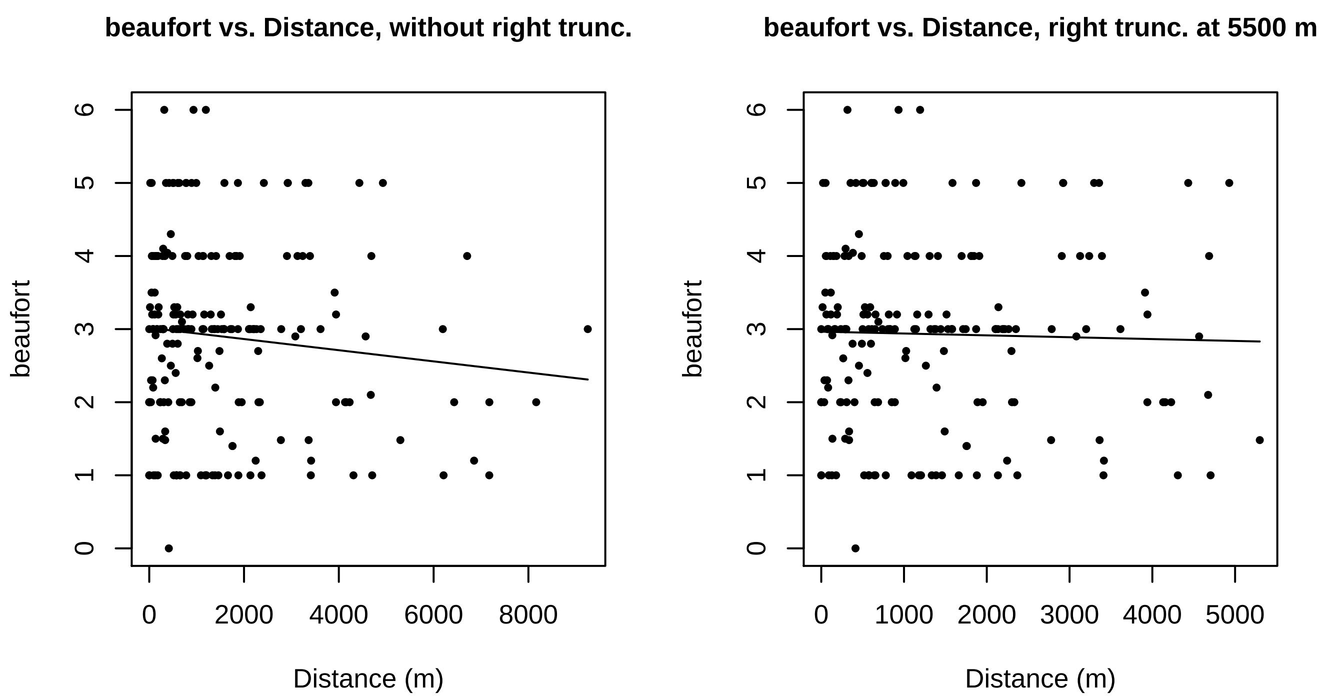

Figure 10: Scatterplots showing the relationship between Beaufort sea state and perpendicular sighting distance, for all sightings (left) and only those not right truncated (right). The line is a simple linear regression.

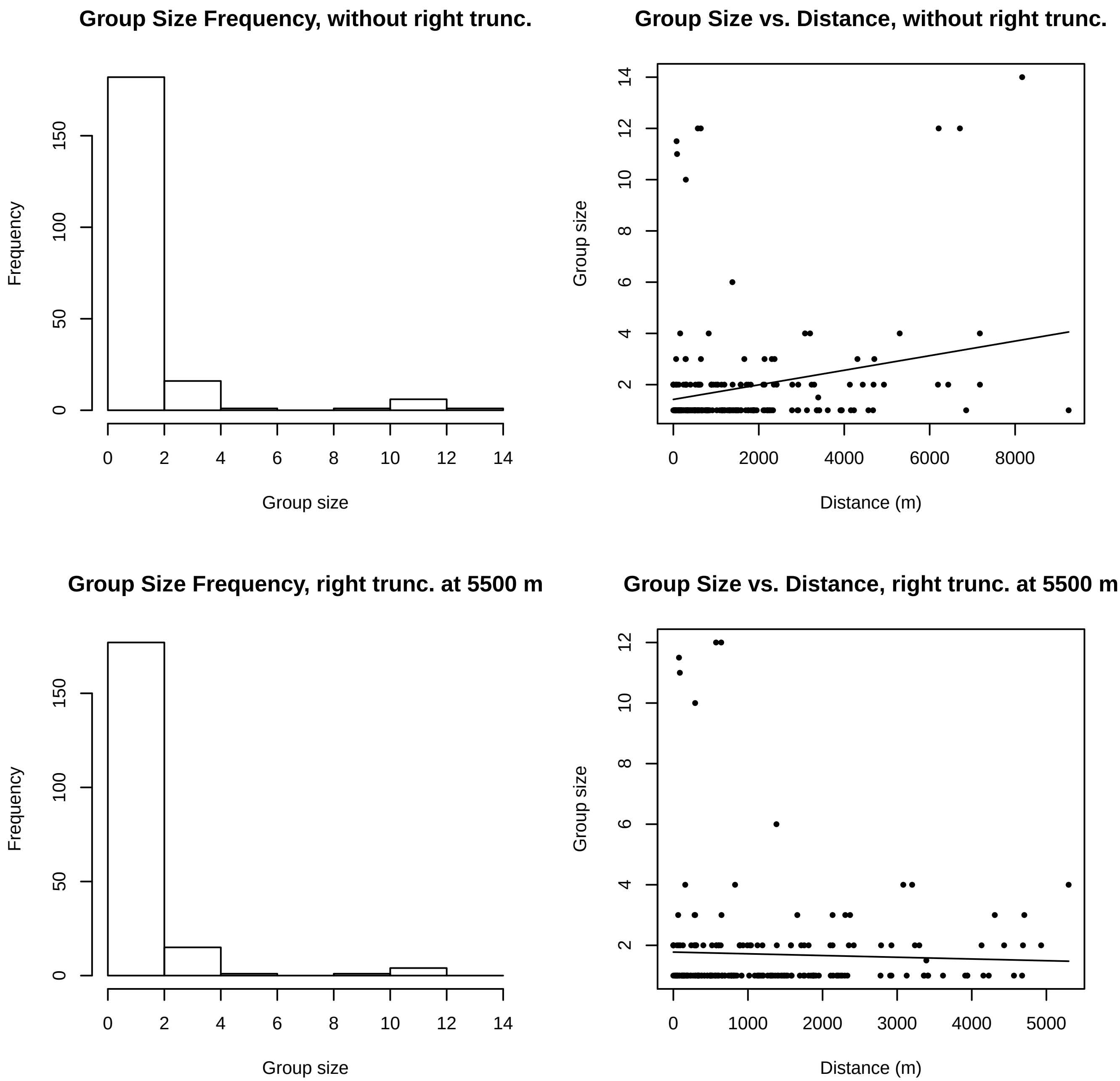

Figure 11: Histograms showing group size frequency and scatterplots showing the relationship between group size and perpendicular sighting distance, for all sightings (top row) and only those not right truncated (bottom row). In the scatterplot, the line is a simple linear regression.

Low Platforms

Because this taxon was sighted too infrequently to fit a detection function to its sightings alone, we fit a detection function to the pooled sightings of several other species that we believed would exhibit similar detectability. These "proxy species" are listed below.

Reported By Observer	Common Name	n
Balaenoptera	Balaenopterid sp.	1
Balaenoptera acutorostrata	Minke whale	3

Balaenoptera borealis	Sei whale	4
Balaenoptera borealis/edeni	Sei or Bryde's whale	5
Balaenoptera borealis/physalus	Fin or Sei whale	0
Balaenoptera edeni	Bryde's whale	7
Balaenoptera musculus	Blue whale	0
Balaenoptera physalus	Fin whale	86
Eubalaena glacialis	North Atlantic right whale	3
Eubalaena glacialis/Megaptera novaeangliae	Right or humpback whale	0
Megaptera novaeangliae	Humpback whale	23
Orcinus orca	Killer whale	12
Total		144

Table 7: Proxy species used to fit detection functions for Low Platforms. The number of sightings, n, is before truncation.

The sightings were right truncated at 5500m.

Covariate	Description
beaufort	Beaufort sea state.
size	Estimated size (number of individuals) of the sighted group.
vessel	Vessel from which the observation was made. This covariate allows the detection function to account for vessel-specific biases, such as the height of the survey platform.

Table 8: Covariates tested in candidate "multi-covariate distance sampling" (MCDS) detection functions.

Key	Adjustment	Order	Covariates	Succeeded	Δ AIC	Mean ESHW (m)
hr				Yes	0.00	1513
hn	cos	2		Yes	0.75	1702
hr	poly	4		Yes	1.76	1486
hr	poly	2		Yes	1.80	1481
hr			vessel	Yes	2.52	1684
hn	cos	3		Yes	11.32	1722
hn			vessel	Yes	13.50	2249
hn			vessel, size	Yes	17.39	2318
hn			size	Yes	17.44	2366
hn				Yes	17.80	2268
hn			beaufort, size	Yes	19.36	2366
hn			beaufort	Yes	19.37	2266
hn	herm	4		No		

hr	beaufort	No
hr	size	No
hn	beaufort, vessel	No
hr	beaufort, vessel	No
hr	beaufort, size	No
hr	vessel, size	No
hn	beaufort, vessel, size	No
hr	beaufort, vessel, size	No

Table 9: Candidate detection functions for Low Platforms. The first one listed was selected for the density model.

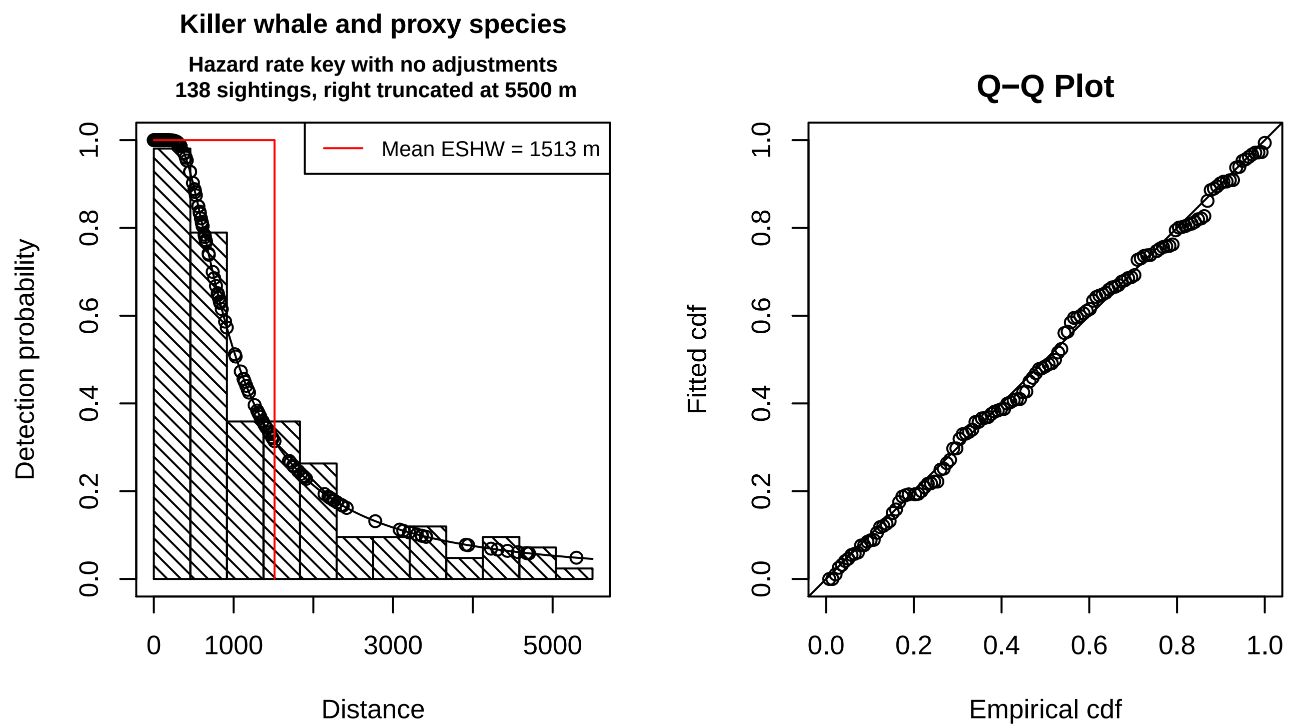

Figure 12: Detection function for Low Platforms that was selected for the density model

Statistical output for this detection function:

```
Summary for ds object
Number of observations :  138
Distance range         :  0  -  5500
AIC                    :  2251.335

Detection function:
 Hazard-rate key function

Detection function parameters
Scale Coefficients:
            estimate        se
```

```
(Intercept) 6.718977 0.2321353

Shape parameters:
            estimate        se
(Intercept) 0.480695 0.1553973

                       Estimate          SE        CV
Average p             0.2751198  0.03724143 0.1353644
N in covered region 501.5996387 77.01845894 0.1535457
```

Additional diagnostic plots:

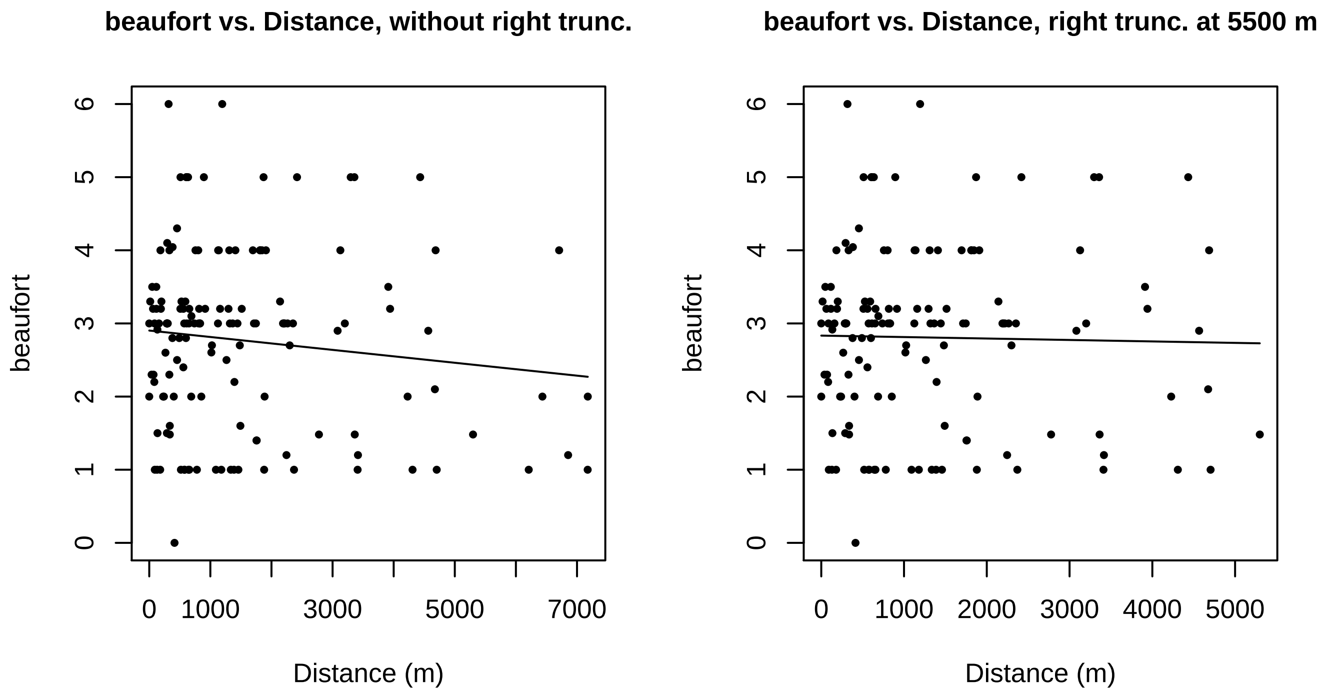

Figure 13: Scatterplots showing the relationship between Beaufort sea state and perpendicular sighting distance, for all sightings (left) and only those not right truncated (right). The line is a simple linear regression.

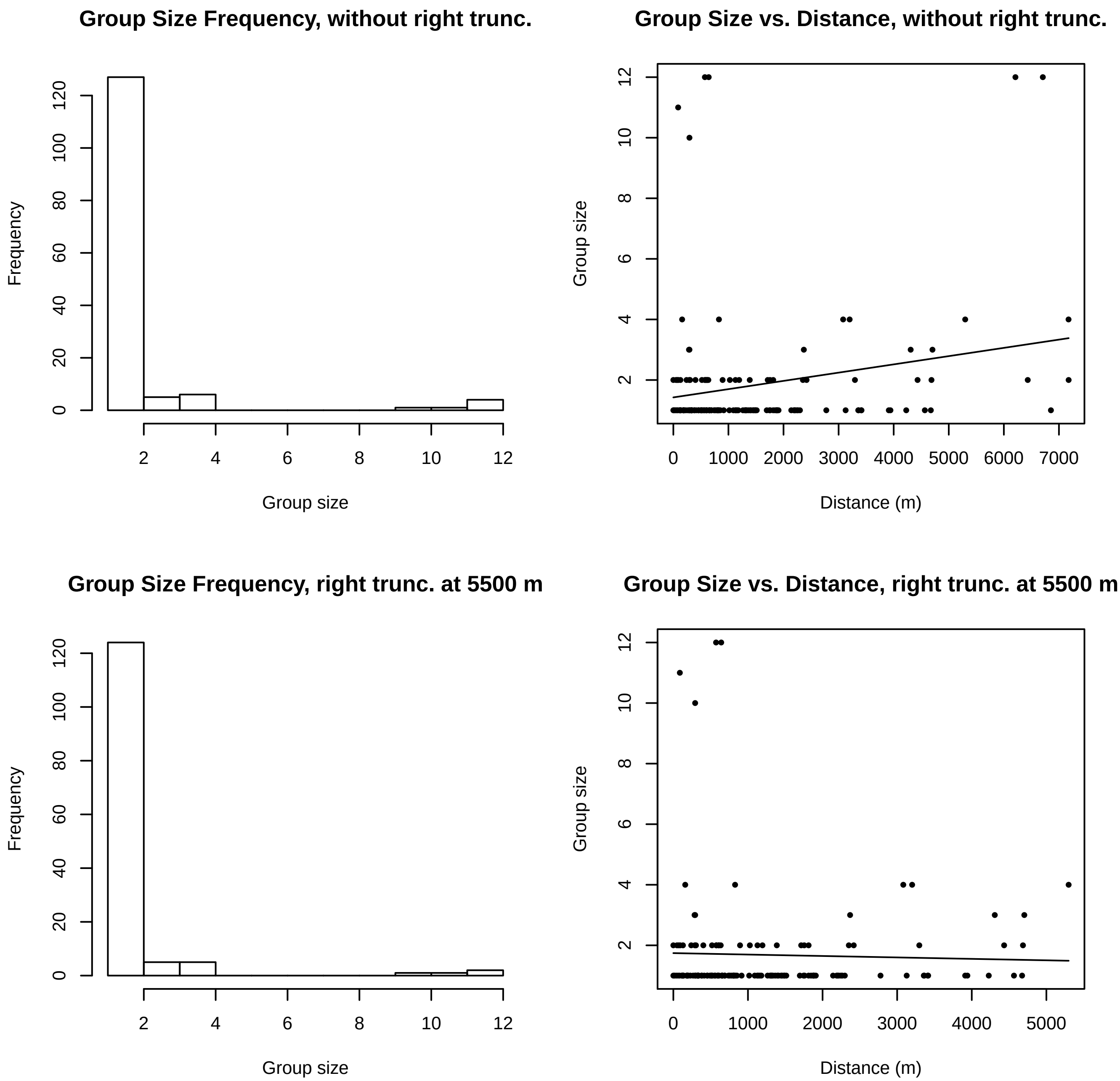

Figure 14: Histograms showing group size frequency and scatterplots showing the relationship between group size and perpendicular sighting distance, for all sightings (top row) and only those not right truncated (bottom row). In the scatterplot, the line is a simple linear regression.

Aerial Surveys

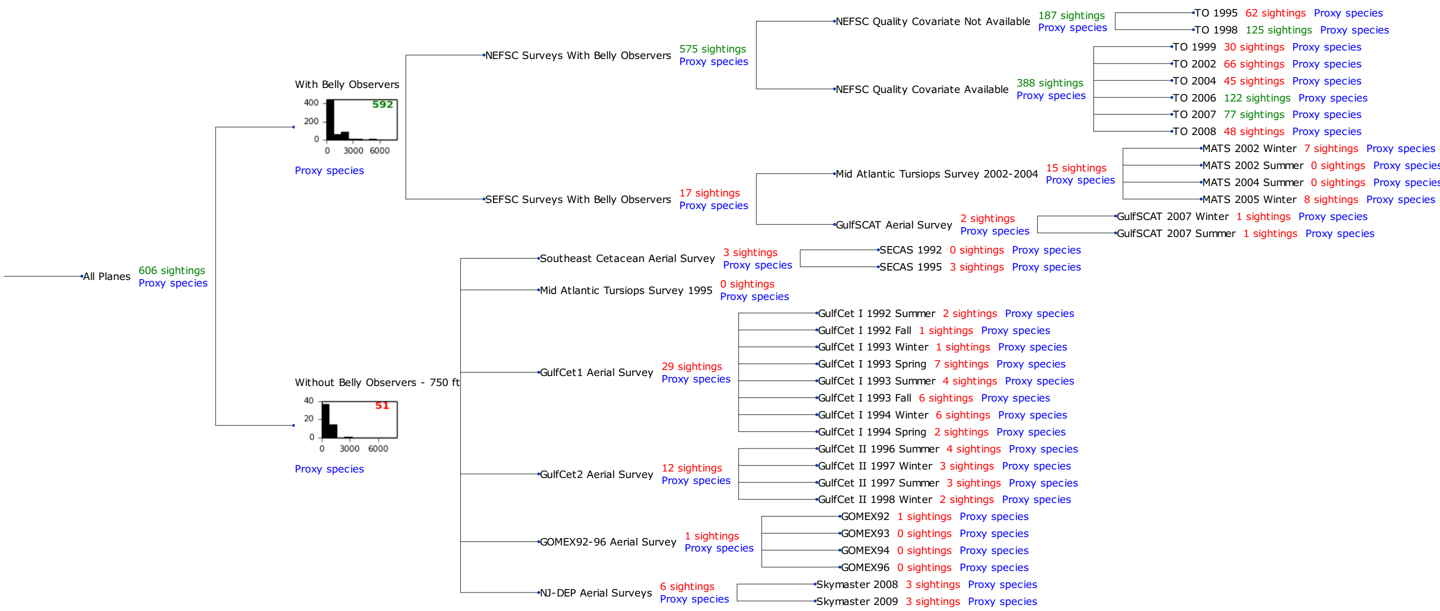

Figure 15: Detection hierarchy for aerial surveys

With Belly Observers

Because this taxon was sighted too infrequently to fit a detection function to its sightings alone, we fit a detection function to the pooled sightings of several other species that we believed would exhibit similar detectability. These "proxy species" are listed below.

Reported By Observer	Common Name	n
Balaenoptera	Balaenopterid sp.	2
Balaenoptera acutorostrata	Minke whale	97
Balaenoptera borealis	Sei whale	14
Balaenoptera borealis/edeni	Sei or Bryde's whale	0
Balaenoptera borealis/physalus	Fin or Sei whale	0
Balaenoptera edeni	Bryde's whale	2
Balaenoptera musculus	Blue whale	1
Balaenoptera physalus	Fin whale	235
Eubalaena glacialis	North Atlantic right whale	43
Eubalaena glacialis/Megaptera novaeangliae	Right or humpback whale	0
Megaptera novaeangliae	Humpback whale	198
Orcinus orca	Killer whale	0
Total		592

Table 10: Proxy species used to fit detection functions for With Belly Observers. The number of sightings, n, is before truncation.

The sightings were right truncated at 2000m.

Covariate	Description
beaufort	Beaufort sea state.
size	Estimated size (number of individuals) of the sighted group.

Table 11: Covariates tested in candidate “multi-covariate distance sampling” (MCDS) detection functions.

Key	Adjustment	Order	Covariates	Succeeded	Δ AIC	Mean ESHW (m)
hn	cos	2		Yes	0.00	594
hr	poly	2		Yes	1.71	598
hr	poly	4		Yes	1.86	609
hr			size	Yes	6.10	632
hr				Yes	7.37	627
hn	cos	3		Yes	11.15	585
hn			size	Yes	22.91	705
hn				Yes	23.39	703
hn	herm	4		No		
hn			beaufort	No		
hr			beaufort	No		
hn			beaufort, size	No		
hr			beaufort, size	No		

Table 12: Candidate detection functions for With Belly Observers. The first one listed was selected for the density model.

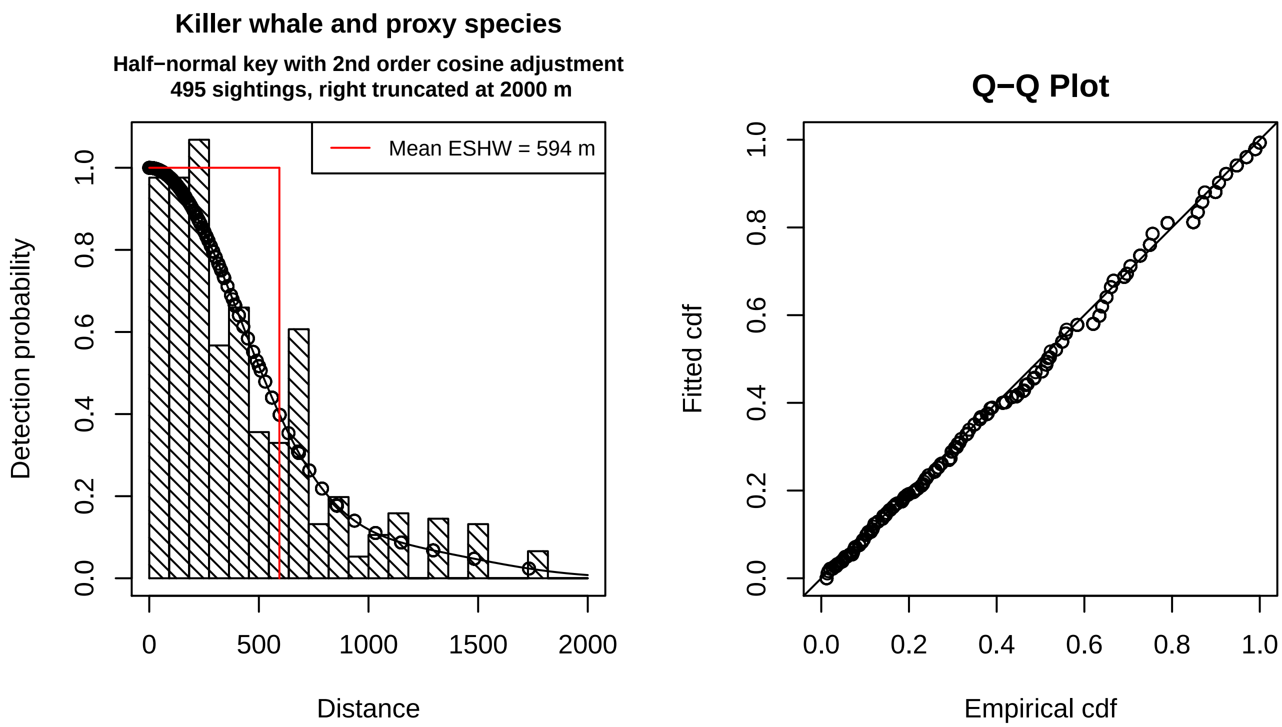

Figure 16: Detection function for With Belly Observers that was selected for the density model

Statistical output for this detection function:

```
Summary for ds object
Number of observations :  495
Distance range         :  0  -  2000
AIC                    :  6960.823

Detection function:
 Half-normal key function with cosine adjustment term of order 2

Detection function parameters
Scale Coefficients:
            estimate        se
(Intercept) 6.464816 0.0431634

Adjustment term parameter(s):
              estimate         se
cos, order 2 0.4286655 0.07975249


Monotonicity constraints were enforced.
                        Estimate          SE         CV
Average p              0.2967564  0.01131843 0.03814046
N in covered region 1668.0347663 89.44444996 0.05362265

Monotonicity constraints were enforced.
```

Additional diagnostic plots:

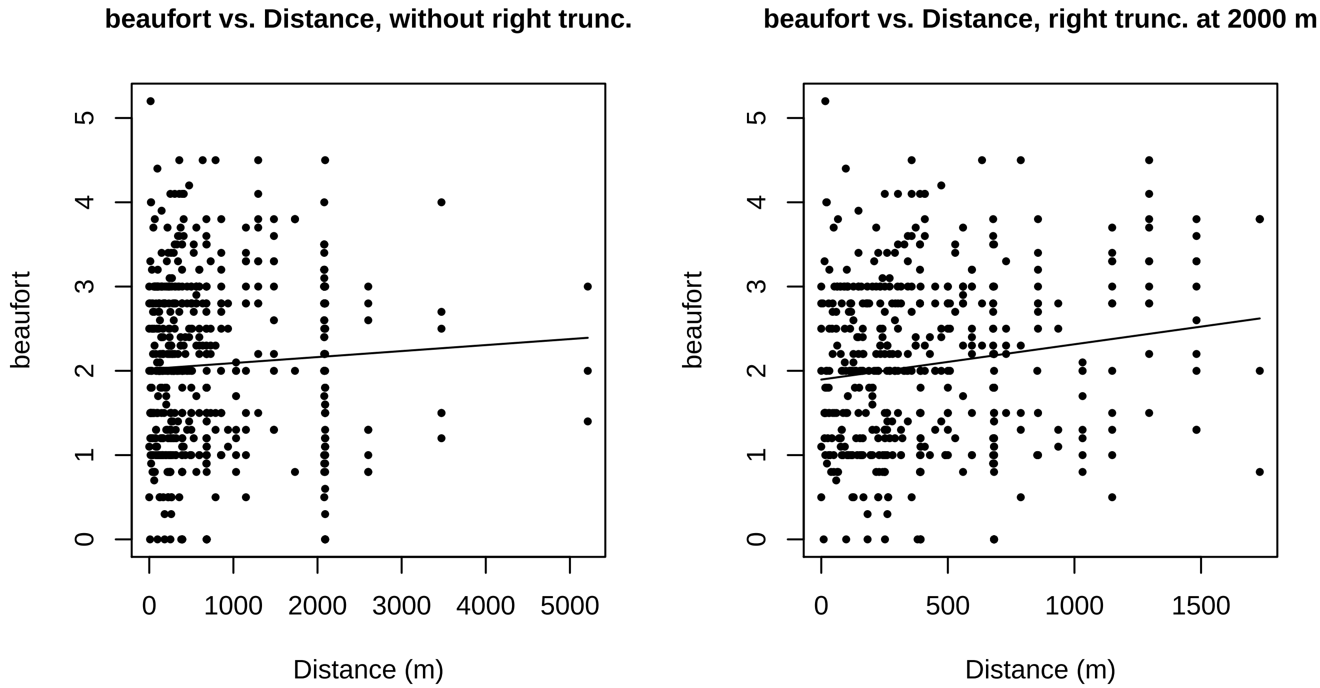

Figure 17: Scatterplots showing the relationship between Beaufort sea state and perpendicular sighting distance, for all sightings (left) and only those not right truncated (right). The line is a simple linear regression.

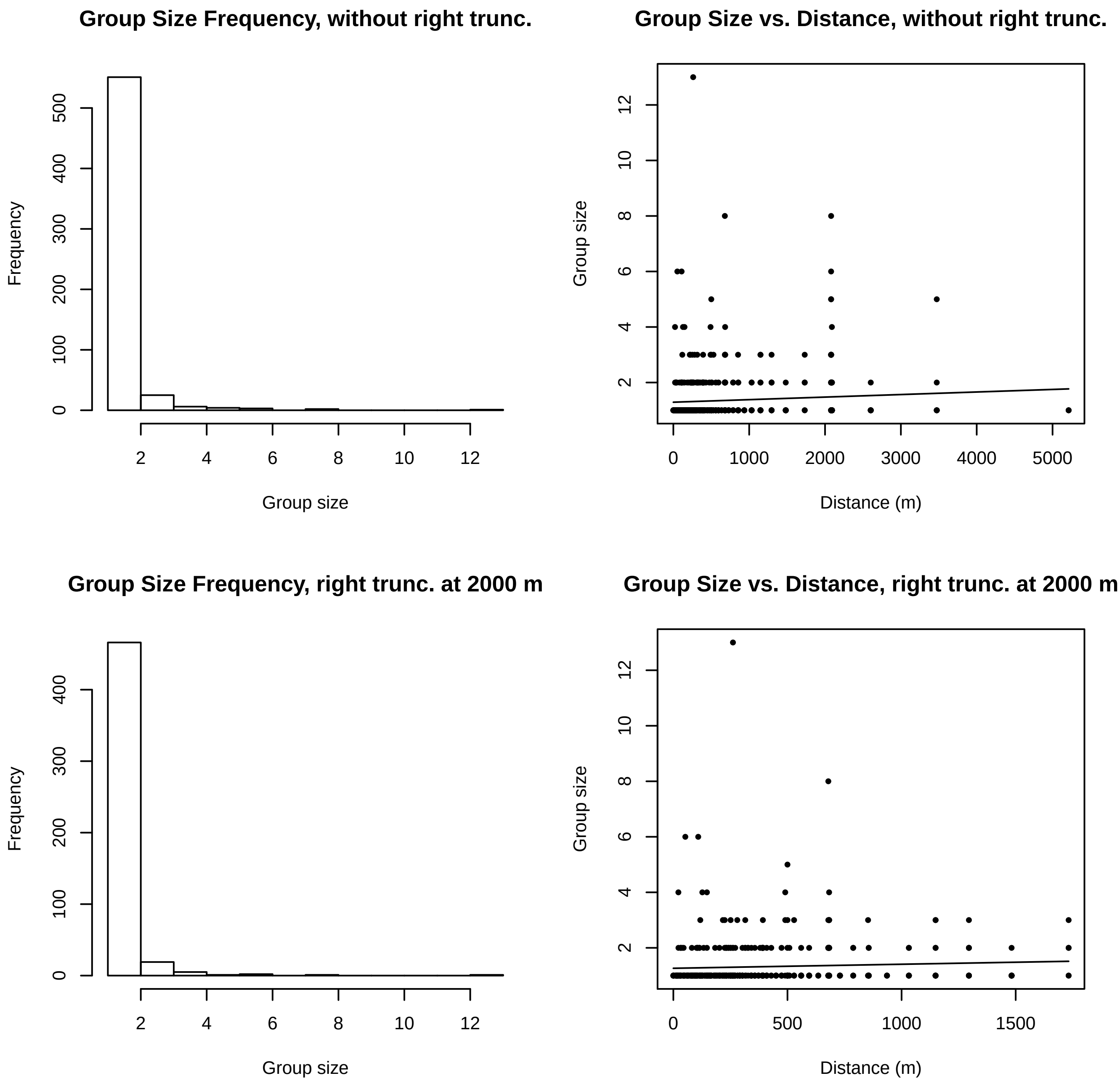

Figure 18: Histograms showing group size frequency and scatterplots showing the relationship between group size and perpendicular sighting distance, for all sightings (top row) and only those not right truncated (bottom row). In the scatterplot, the line is a simple linear regression.

Without Belly Observers - 750 ft

Because this taxon was sighted too infrequently to fit a detection function to its sightings alone, we fit a detection function to the pooled sightings of several other species that we believed would exhibit similar detectability. These "proxy species" are listed below.

Reported By Observer	Common Name	n
Balaenoptera	Balaenopterid sp.	1
Balaenoptera acutorostrata	Minke whale	0

Balaenoptera borealis	Sei whale	0
Balaenoptera borealis/edeni	Sei or Bryde's whale	2
Balaenoptera borealis/physalus	Fin or Sei whale	0
Balaenoptera edeni	Bryde's whale	3
Balaenoptera musculus	Blue whale	0
Balaenoptera physalus	Fin whale	2
Eubalaena glacialis	North Atlantic right whale	0
Eubalaena glacialis/Megaptera novaeangliae	Right or humpback whale	0
Megaptera novaeangliae	Humpback whale	6
Orcinus orca	Killer whale	0
Physeter macrocephalus	Sperm whale	37
Total		51

Table 13: Proxy species used to fit detection functions for Without Belly Observers - 750 ft. The number of sightings, n, is before truncation.

The sightings were right truncated at 600m. Due to a reduced frequency of sightings close to the trackline that plausibly resulted from the behavior of the observers and/or the configuration of the survey platform, the sightings were left truncted as well. Sightings closer than 40 m to the trackline were omitted from the analysis, and it was assumed that the the area closer to the trackline than this was not surveyed. This distance was estimated by inspecting histograms of perpendicular sighting distances. The vertical sighting angles were heaped at 10 degree increments, so the candidate detection functions were fitted using linear bins scaled accordingly.

Key	Adjustment	Order	Covariates	Succeeded	Δ AIC	Mean ESHW (m)
hn	cos	2		Yes	0.00	216
hr				Yes	0.59	251
hn	cos	3		Yes	2.31	255
hn	herm	4		Yes	2.46	316
hr	poly	2		Yes	2.59	251
hr	poly	4		Yes	2.72	252
hn				No		

Table 14: Candidate detection functions for Without Belly Observers - 750 ft. The first one listed was selected for the density model.

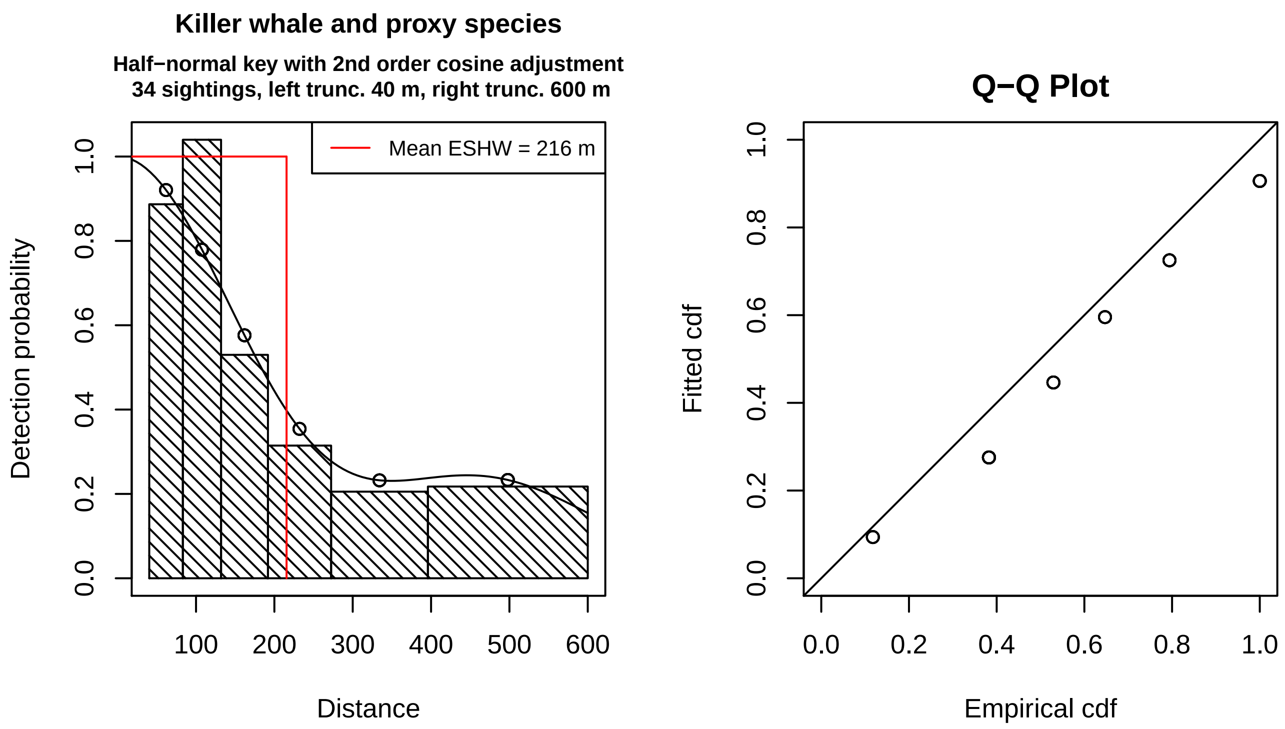

Figure 19: Detection function for Without Belly Observers - 750 ft that was selected for the density model

Statistical output for this detection function:

```
Summary for ds object
Number of observations :  34
Distance range         :  40.30835  -  600
AIC                    :  124.984

Detection function:
 Half-normal key function with cosine adjustment term of order 2

Detection function parameters
Scale Coefficients:
            estimate        se
(Intercept) 5.738324 0.1838281

Adjustment term parameter(s):
              estimate       se
cos, order 2 0.4333817 0.242253


Monotonicity constraints were enforced.
                      Estimate          SE        CV
Average p            0.3592781  0.08709339 0.2424122
N in covered region 94.6342010 26.36346821 0.2785829

Monotonicity constraints were enforced.
```

Additional diagnostic plots:

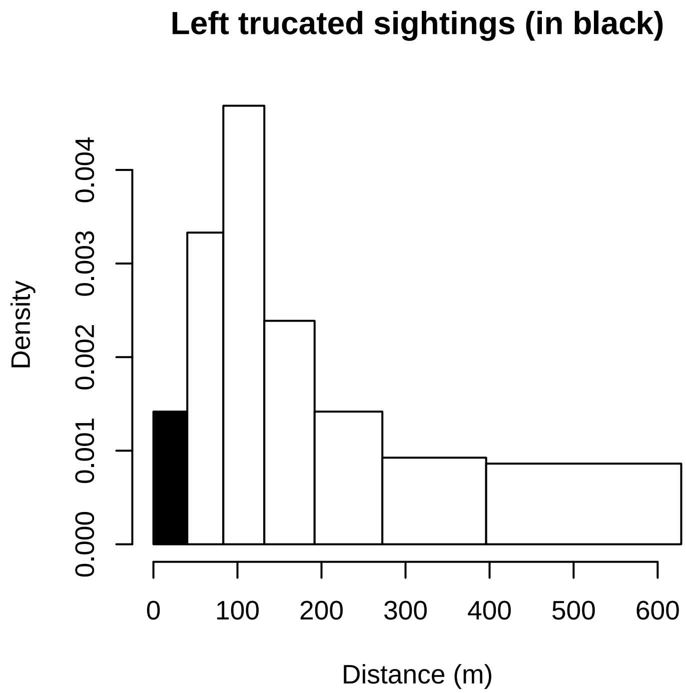

Figure 20: Density of sightings by perpendicular distance for Without Belly Observers - 750 ft. Black bars on the left show sightings that were left truncated.

g(0) Estimates

Platform	Surveys	Group Size	*g(0)*	Biases Addressed	Source
Shipboard	All	Any	0.921	Perception	Barlow and Forney (2007)
Aerial	All	Any	0.78	Availability	Hooker et al. (2012)

Table 15: Estimates of *g(0)* used in this density model.

No species- or survey-specific estimates of g(0) were available for killer whales for any surveys in our study. For shipboard surveys, we used Barlow and Forney's (2007) estimate (0.921) for large whales (including killer whales) produced from several years of dual-team surveys in the Pacific ocean that used similar binoculars and protocols to the binocular surveys in our study. We also applied this estimate to the naked eye surveys in our study, as we found no estimate of g(0) in the literature for killer whales observed by naked eye from shipboard surveys.

This estimate accounted for perception bias but not availability bias, but we do not believe availability to be a major factor affecting detectability of killer whales from shipboard surveys, as they are not a particularly long-diving species. For long diving cetaceans such as sperm whales, Kogia spp., and beaked whales, Barlow and Forney (2007) used Barlow's (1999) model of g(0) that incorporated dive behavior. Barlow parameterized that model such that the median duration of long dives ranged from 10.9-28.6 min, depending on the species, based on prior observational studies. By comparison, Baird et al. (2005) reported that mean dive durations for 41 fish-eating killer whales for dives >= 1 min in duration was 2.3-2.4 min. Miller et al. (2010) studied the diving behavior of 12 mammal-eating killer whales, which exhibited longer dives. The authors did not report dive duration statistics but noted that the whales spent 50% of their time 8 m or shallower and 90% of their time 40 m or shallower. Hooker et al. (2012) reported that unspecified killer whales spent 78% of their time between 0-10 m. Finally, Sivle et al. (2012) characterized killer whales as a "shallow-diving" odontocete; by contrast, they characterized pilot whales as "intermediate diving" and sperm whales as "deep diving" odontocetes.

We did not find a species-specific g(0) estimate for killer whales observed by aircraft in the literature. Palka (2006) estimated of g(0) for groups of 1-5 large whales from from two years of aerial surveys using the Hiby (1999) circle- back method. This estimate accounted for both availability and perception bias, but pooled sightings of several species together to provide a generic estimate for all large whales, due to sample-size limitations. Most of these species undertake longer dives than killer whales; we believe Palka's g(0) was dominated by availability bias of such species and thus underestimates killer whale detectability. Instead, we used Hooker et al.'s (2012) report that an unspecified number and type of killer whales spent 78% of time between 0-10 m and set g(0)=0.78.

We note that percent time spent at 0-10 m does not necessarily equate to "percent time detectable by aerial observation". Hooker et al.'s data appear to be those reported by Kvadsheim et al. (2012). The four killer whales monitored in that study performed roughly 20x more dives to 1-30 m than to 30-200 m; the mean depth of the 1-30 m dives was only 2.6-3.6 m.

Density Model

Killer whales are widely distributed throughout the world's oceans and are found in tropical, temperate, and high-latitude waters, in both pelagic and coastal habitats (Forney and Wade 2006). They are considered rare in the Gulf of Mexico, U.S. Atlantic waters, and the Bay of Fundy, uncommon but seasonally regular in Labrador and Newfoundland, and common in the Canadian Arctic (Forney and Wade 2006). In the Gulf of Mexico, the NOAA surveys from 1992-2009 utilized here only reported 16 sightings.

A recent comprehensive analysis of available systematic and opportunistic sightings in the northwest Atlantic between 40-60 N, 40-75 W reported that almost all of the sightings in this region occurred at depths less than 200m (Lawson and Stevens 2014). These authors noted, however, that this might reflect a bias in the distribution of observation effort, and that killer whales have been reported in mid-Atlantic waters at depths exceeding 3000m. The 16 sightings reported by the NOAA surveys in the Gulf of Mexico were in waters ranging from 547-3367m. Sightings of killer whales in the northern Gulf of Mexico during 1921-1995 occurred primarily in waters ranging from 256-2652m, and no killer whales have been reported in shelf waters other than in 1921, 1985, and 1987 (Waring et al. 2013).

Given this evidence that killer whales do not inhabit shelf waters of the Gulf of Mexico, we contemplated the best way to exclude this area of absence from our models. Normally, with only 16 sightings, we would not consider fitting a spatial model using a regression of habitat variables, but instead estimate mean density over the region we presumed the modeled taxon occupied. But of all the oceanic cetaceans we modeled in the Gulf of Mexico, killer whales were the species sighted most frequently far from the shelf and closest to the deep waters of the central Gulf. Rather than split the study area at the shelf break and assume, in essence, that killer whales were equally likely to inhabit all off-shelf waters, as we did for some other species, we instead fitted a regression model to all segments with the logarithm of depth as the single covariate, to allow the data to determine how best to relate killer whale density to depth.

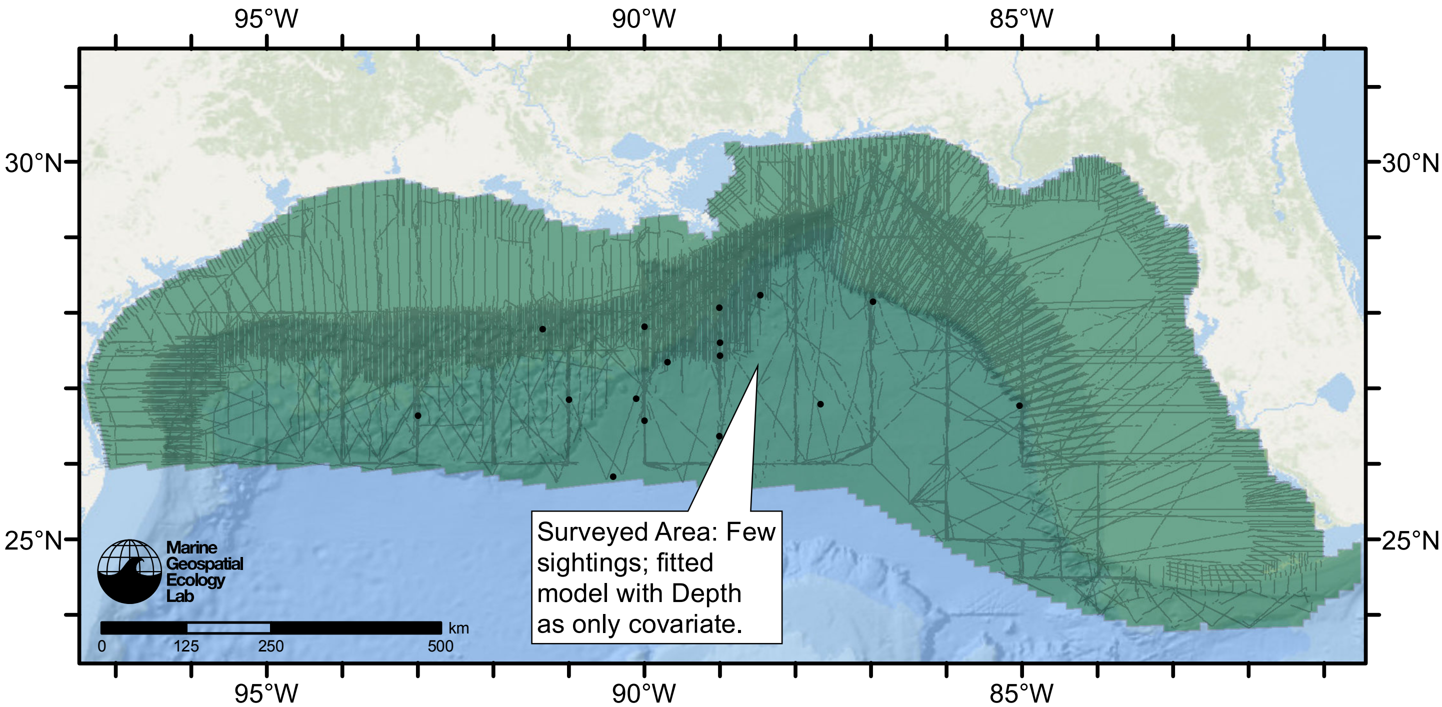

Figure 21: Killer whale density model schematic. All on-effort sightings are shown, including those that were truncated when detection functions were fitted.

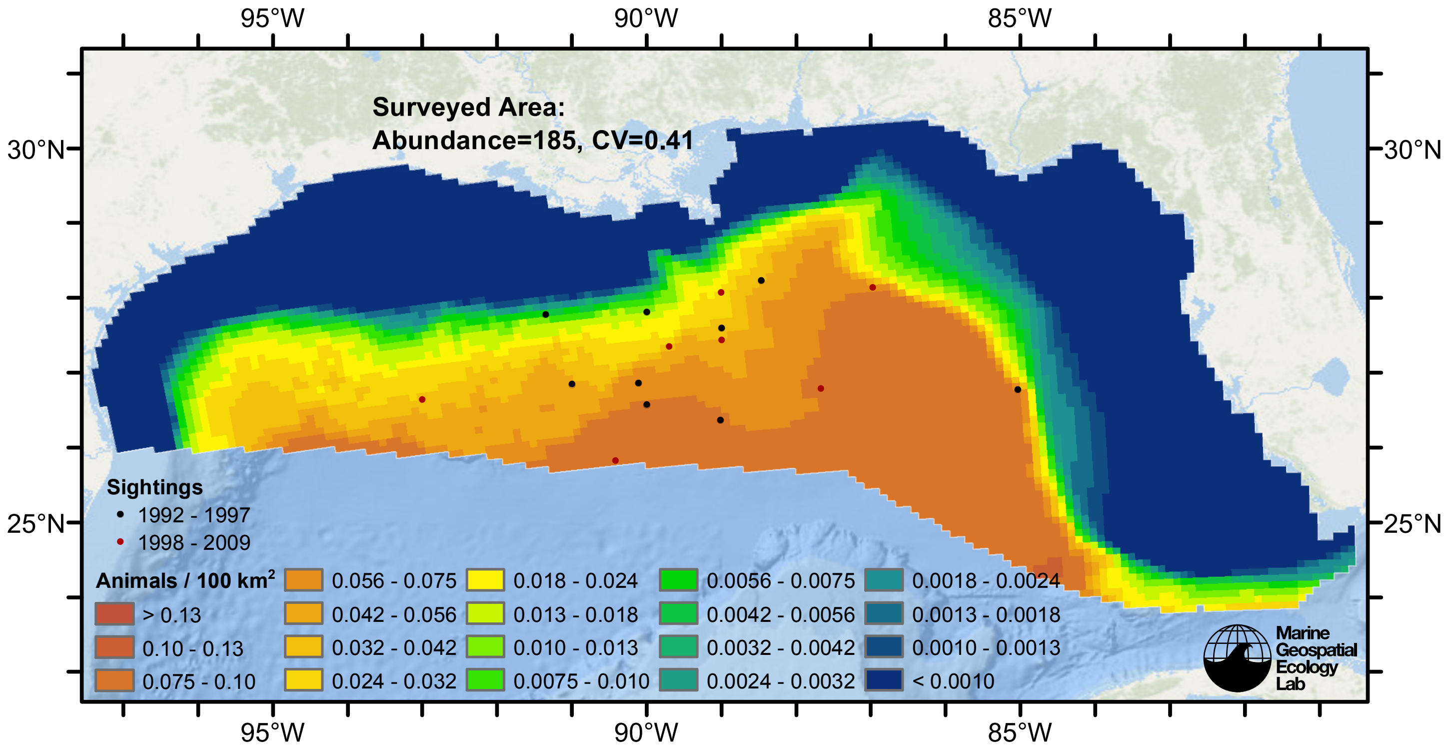

Figure 22: Killer whale density predicted by the climatological model that explained the most deviance. Pixels are 10x10 km. The legend gives the estimated individuals per pixel; breaks are logarithmic. Abundance for each region was computed by summing the density cells occuring in that region.

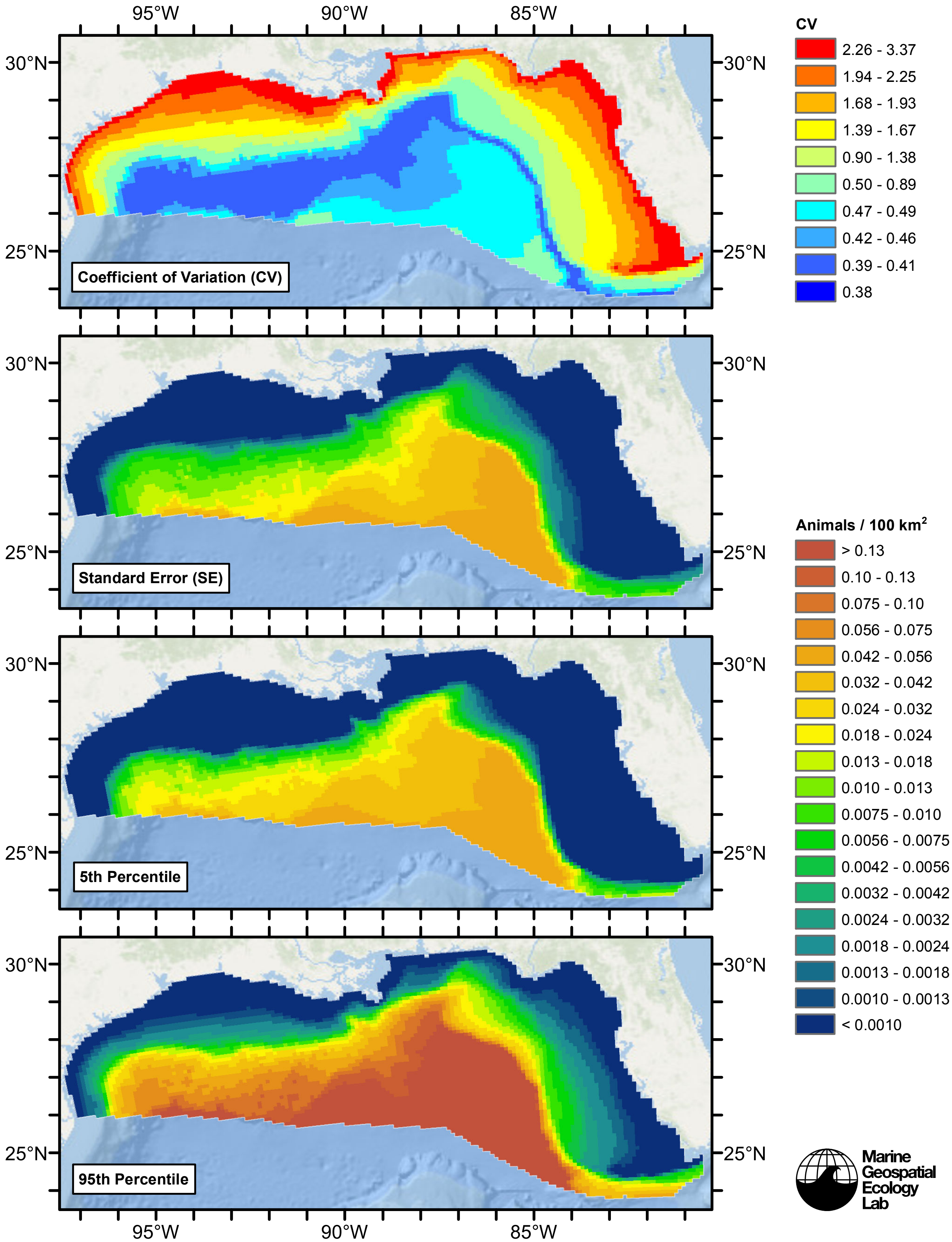

Figure 23: Estimated uncertainty for the climatological model that explained the most deviance. These estimates only incorporate the statistical uncertainty estimated for the spatial model (by the R mgcv package). They do not incorporate uncertainty in the detection functions, g(0) estimates, predictor variables, and so on.

Surveyed Area

Statistical output

```
Rscript.exe: This is mgcv 1.8-2. For overview type 'help("mgcv-package")'.


Family: Tweedie(p=1.384)
Link function: log

Formula:
abundance ~ offset(log(area_km2)) + s(log10(Depth), bs = "ts",
    k = 5)

Parametric coefficients:
            Estimate Std. Error t value Pr(>|t|)
(Intercept)  -10.345      0.873  -11.85   <2e-16 ***
---
Signif. codes:  0 '***' 0.001 '**' 0.01 '*' 0.05 '.' 0.1 ' ' 1

Approximate significance of smooth terms:
                   edf Ref.df     F p-value
s(log10(Depth)) 0.9699      4 2.425 0.00121 **
---
Signif. codes:  0 '***' 0.001 '**' 0.01 '*' 0.05 '.' 0.1 ' ' 1

R-sq.(adj) =  -0.000168   Deviance explained = 29.8%
-REML =  140.9  Scale est. = 140.33    n = 19881

All predictors were significant. This is the final model.
Creating term plots.
Diagnostic output from gam.check():

Method: REML   Optimizer: outer newton
full convergence after 12 iterations.
Gradient range [-1.267699e-06,7.900794e-07]
(score 140.9004 & scale 140.331).
Hessian positive definite, eigenvalue range [0.3580042,78.9467].
Model rank =  5 / 5

Basis dimension (k) checking results. Low p-value (k-index<1) may
indicate that k is too low, especially if edf is close to k'.

                   k'   edf k-index p-value
s(log10(Depth)) 4.000 0.970   0.783       0

Predictors retained during the model selection procedure: Depth

Predictors dropped during the model selection procedure:
```

Model term plots

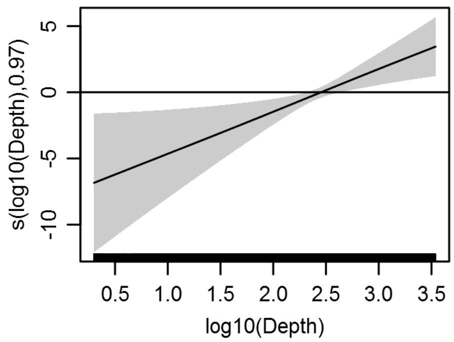

Diagnostic plots

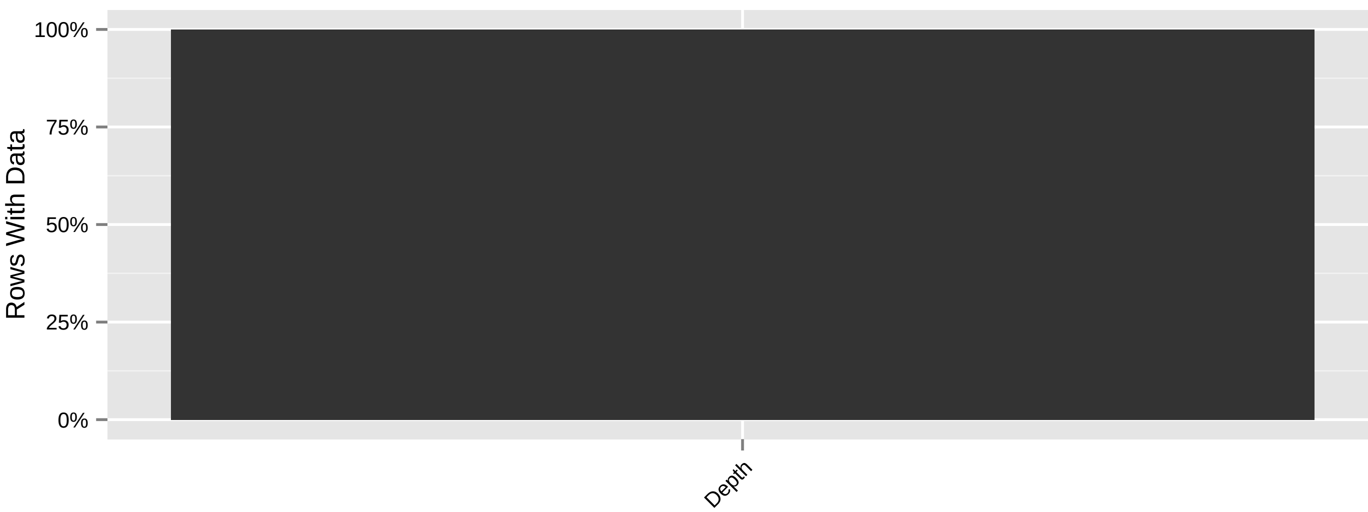

Figure 24: Segments with predictor values for the Killer whale Climatological model, Surveyed Area. This plot is used to assess how many segments would be lost by including a given predictor in a model.

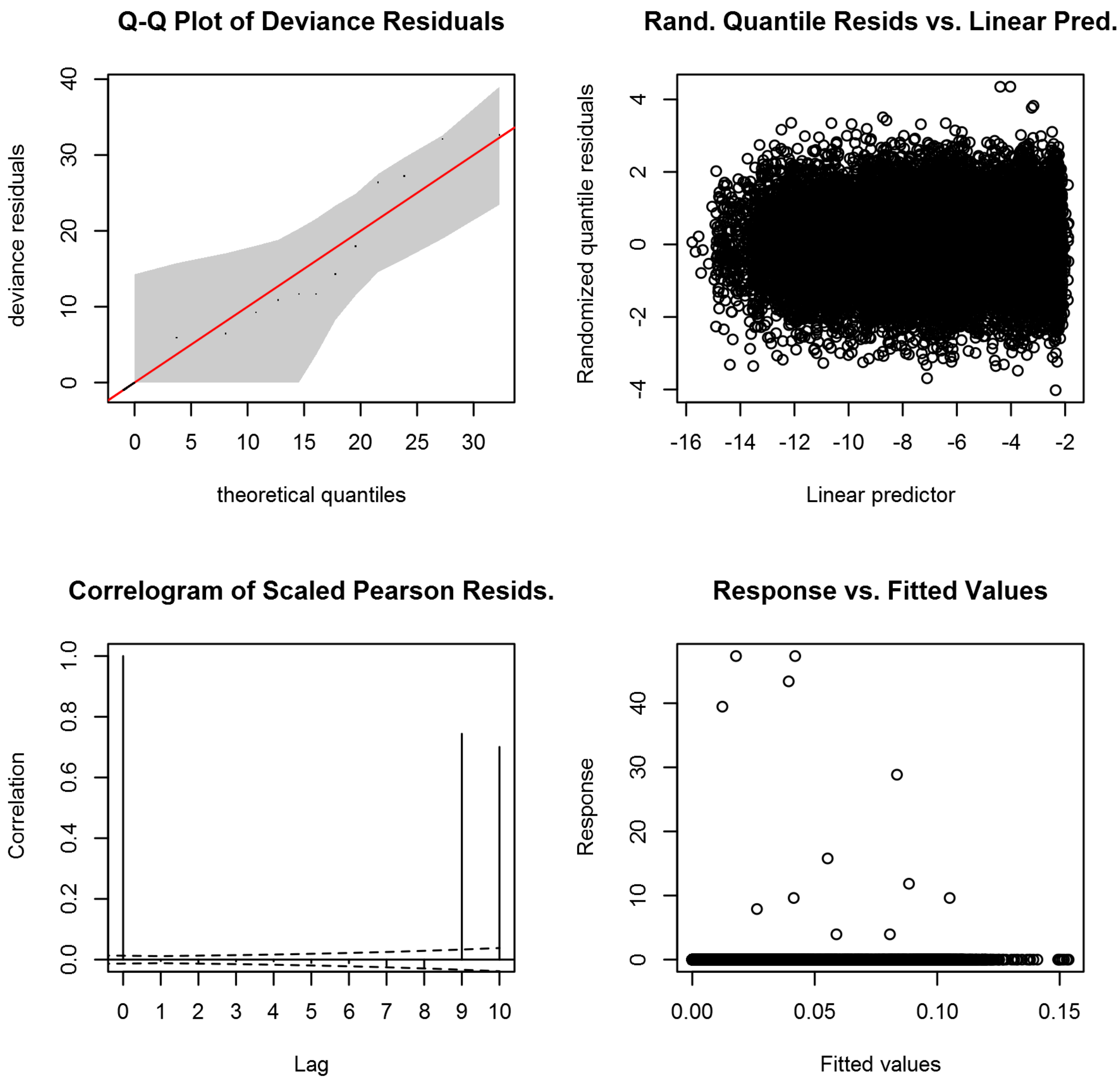

Figure 25: Statistical diagnostic plots for the Killer whale Climatological model, Surveyed Area.

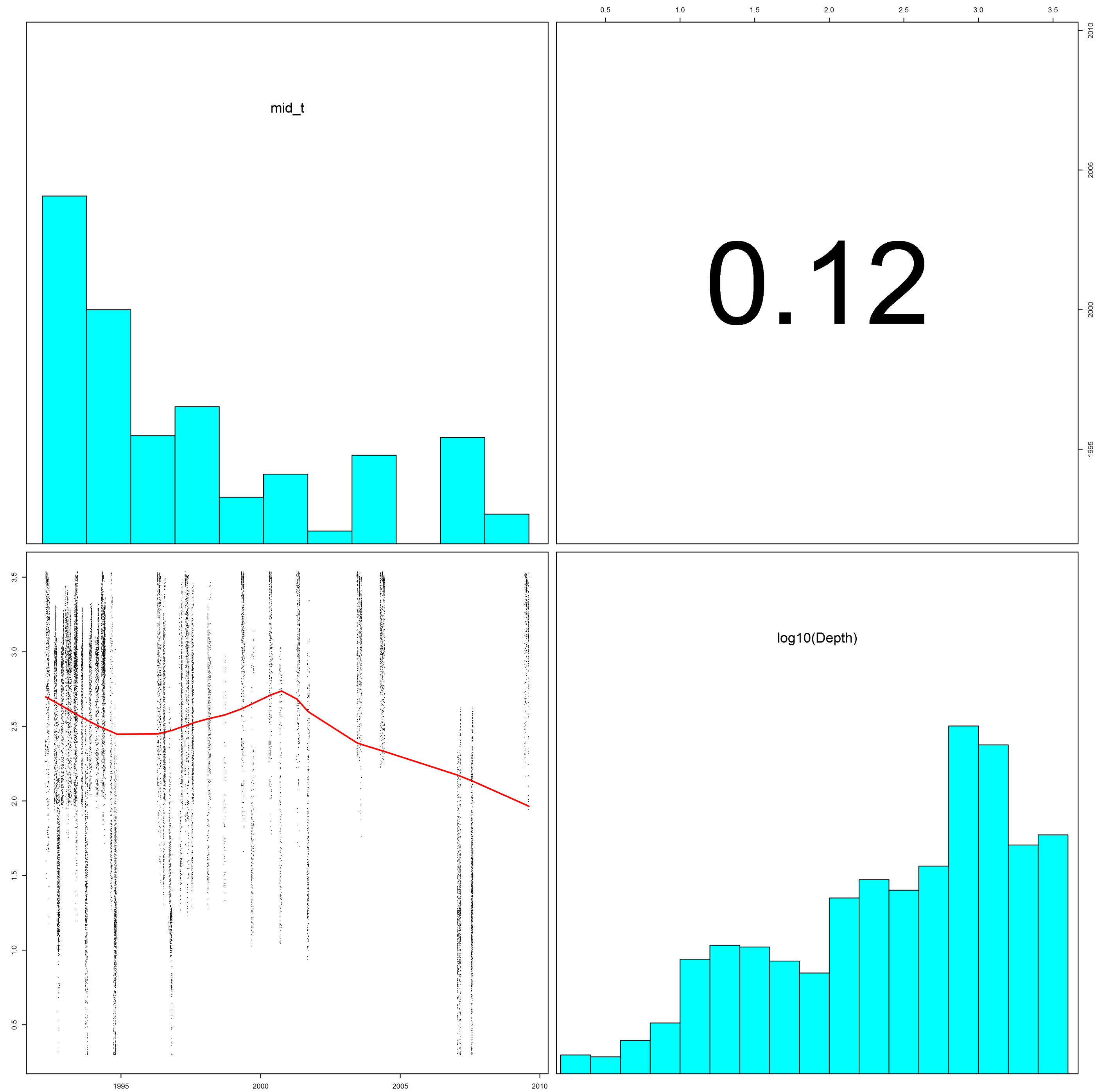

Figure 26: Scatterplot matrix for the Killer whale Climatological model, Surveyed Area. This plot is used to inspect the distribution of predictors (via histograms along the diagonal), simple correlation between predictors (via pairwise Pearson coefficients above the diagonal), and linearity of predictor correlations (via scatterplots below the diagonal). This plot is best viewed at high magnification.

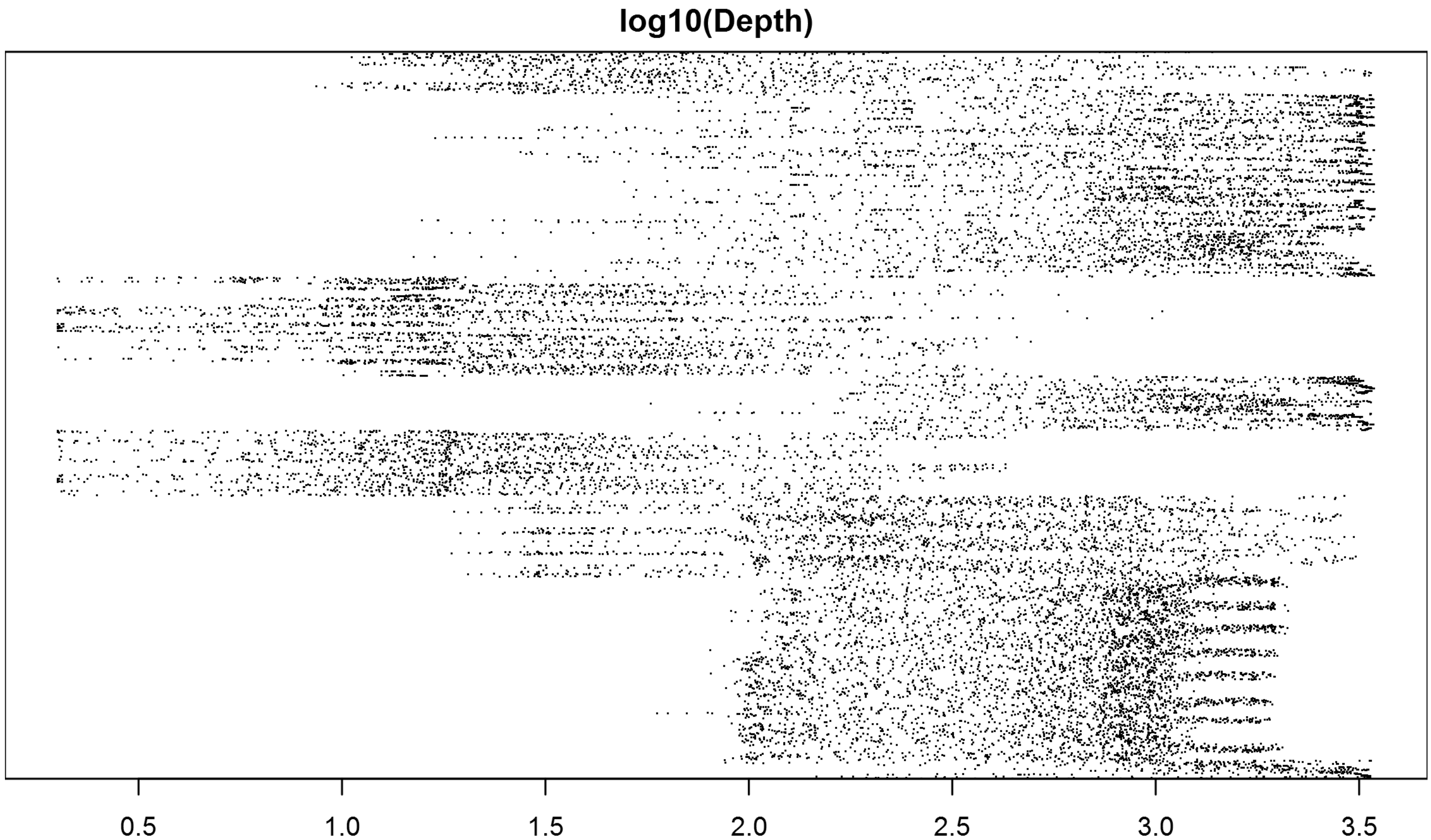

Figure 27: Dotplot for the Killer whale Climatological model, Surveyed Area. This plot is used to check for suspicious patterns and outliers in the data. Points are ordered vertically by transect ID, sequentially in time.

Model Comparison

Abundance Estimates

The table below shows the estimated mean abundance (number of animals) within the study area. The Assumed g(0)=1 column specifies whether the abundance estimate assumed that detection was certain along the survey trackline. Studies that assumed this did not correct for availability or perception bias, and therefore underestimated abundance. The In our models column specifies whether the survey data from the study was also used in our models. If not, the study provides a completely independent estimate of abundance.

Dates	Model or study	Estimated abundance	CV	Assumed g(0)=1	In our models
1992-2009	Climatological model	185	0.41	No	
2009	Oceanic waters, Jun-Aug (Waring et al. 2013)	28	1.02	Yes	Yes
2003-2004	Oceanic waters, Jun-Aug (Mullin 2007)	49	0.77	Yes	Yes
1996-2001	Oceanic waters, Apr-Jun (Mullin and Fulling 2004)	133	0.49	Yes	Yes
1991-1994	Oceanic waters, Apr-Jun (Hansen et al. 1995)	277	0.42	Yes	Yes

Table 16: Estimated mean abundance within the study area. For comparison, independent abundance estimates from NOAA technical reports and/or the scientific literature are shown. Please see the Discussion section below for our evaluation of our models compared to the other estimates. Note that our abundance estimates are averaged over the whole year, while the other studies may have estimated abundance for specific months or seasons. Our coefficients of variation (CVs) underestimate the true uncertainty in our estimates, as they only incorporated the uncertainty of the GAM stage of our models. Other sources of uncertainty include the detection functions and g(0) estimates. It was not possible to incorporate these into our CVs without undertaking a computationally-prohibitive bootstrap; we hope to attempt that in a future version of our models.

Density Map

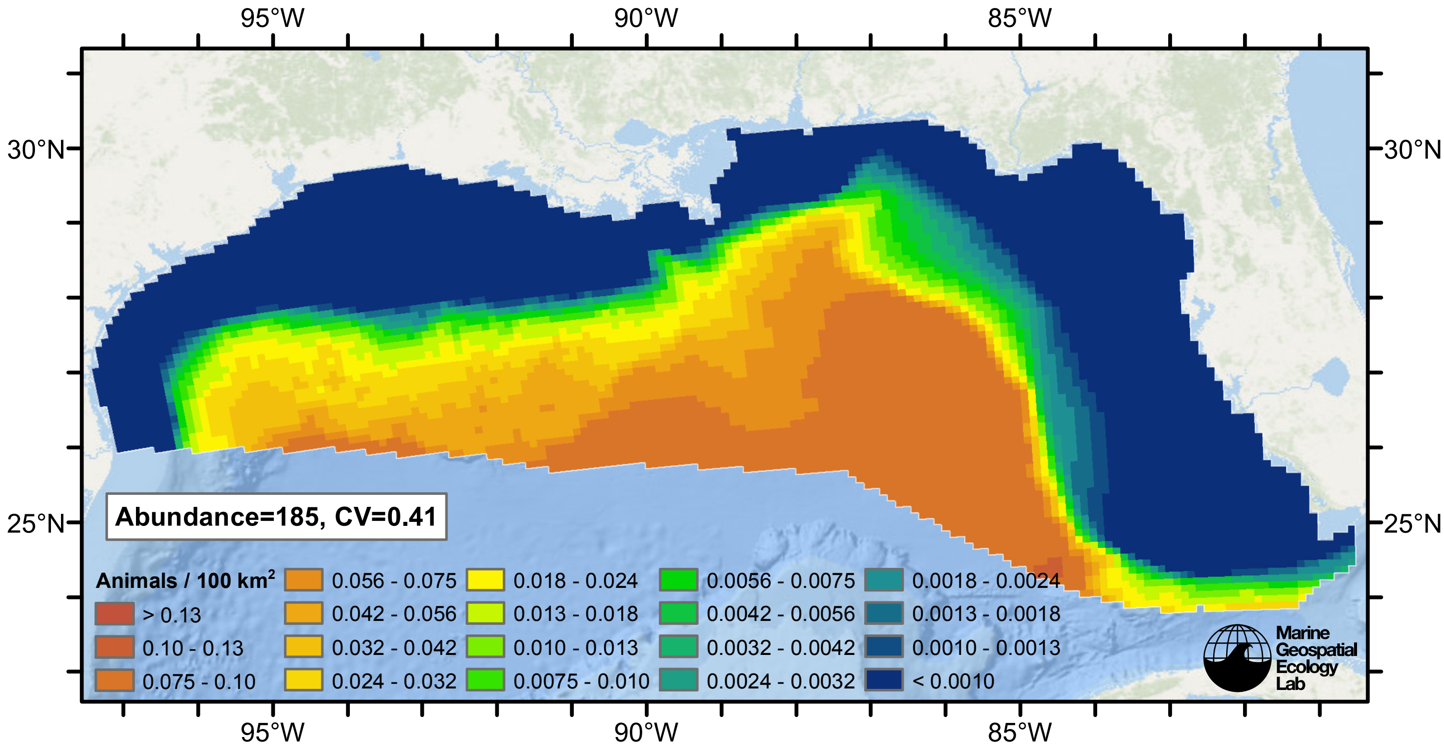

Figure 28: Killer whale density and abundance predicted by the climatological predictor model. Regions inside the study area (white line) where the background map is visible are areas we did not model (see text).

Discussion

The statistical modeling software, mgcv, determined that there was a statistically-significant relationship between density and depth and fitted a linear model, although this should be viewed cautiously given that the model was built from only 16 sightings. Predicted across the study area, this model estimated an abundance of 185. NOAA made a series of four abundance estimates that steadily decreased from 277 for 1991-1994 to 28 in 2009. NOAA cautioned that although the estimates show a steady decrease the data are not sufficient to infer a statistically-significant decreasing trend in population size (Waring et al. 2013). In any case, our estimate of 185 falls roughly in the middle of the range of NOAA's estimates, which seems reasonable given that it was built from a pooling of all of the data NOAA used to make the series of four estimates.

At the time of this writing, NOAA's most recent abundance estimate of 28 is what NOAA used to estimate stock-level parameters important to management, including the Minimum Population Estimate (Nmin) and the Potential Biological Removal (PBR). Because this estimate is very low relative to the abundance we estimated, it is likely that if our results are used to estimate population-level impacts from potentially harmful human activities (i.e. "takes", as defined by the Marine Mammal Protection Act), the estimated impacts will be very high relative NOAA's estimated stock size (i.e. the estimated takes will greatly exceed PBR).

There is no easy solution to this problem. One possibility is that NOAA could recalculate stock-level parameters such as Nmin and PBR using our results. But this would violate NOAA's guideline that data older than 8 years not be used to estimate stock-level parameters (Moore et al. 2011). Alternatively, impacts could be estimated using NOAA's abundance estimate of 28, computing density by dividing this number by the total area of the off-shelf portion of the U.S. Exclusive Economic Zone in the Gulf of Mexico. But this would fail to account for the non-uniform distribution of killer whales predicted by our study (although our model of this distribution was based on just 16 sightings, so it should be viewed cautiously.) Finally, in a hybrid approach, a new density surface could be obtained by apportioning NOAA's abundance estimate of 28 proportionally according to the density surface predicted by our models. To do that, divide our density surface by our total estimated abundance (185), then multiply every cell by 28. To check that the result computed correctly, sum up all of the cells; the result should equal 28. This new density surface would reflect the distribution pattern predicted by our study but use the total abundance estimate from NOAA.

Interested parties should consult with NOAA about the best way to proceed with this problem.

References

Baird RW, Hanson MB, Dill LM (2005) Factors influencing the diving behaviour of fish-eating killer whales: sex differences and diel and interannual variation in diving rates. Can J Zool. 83: 257-267.

Barlow J (1999) Trackline detection probability for long diving whales. In: Marine Mammal Survey and Assessment Methods (Garner GW, Amstrup SC, Laake JL, Manly BFJ, McDonald LL, Robertson DG, eds.). Balkema, Rotterdam, pp. 209-221.

Barlow J, Forney KA (2007) Abundance and density of cetaceans in the California Current ecosystem. Fish. Bull. 105: 509-526.

Forney KA, Wade PR (2007) Worldwide Distribution and Abundance of Killer Whales. In: Whales, whaling and ocean ecosystems (Estes JA, DeMaster DP, Doak DF, Williams TM, Brownell RL, eds). University of California Press, Berkeley, California. pp. 145-162.

Hansen LJ, Mullin KD, Roden CL (1995) Estimates of cetacean abundance in the northern Gulf of Mexico from vessel surveys. Southeast Fisheries Science Center, Miami Laboratory, Contribution No. MIA-94/95-25, 9 pp.

Hiby L (1999) The objective identification of duplicate sightings in aerial survey for porpoise. In: Marine Mammal Survey and Assessment Methods (Garner GW, Amstrup SC, Laake JL, Manly BFJ, McDonald LL, Robertson DG, eds.). Balkema, Rotterdam, pp. 179-189.

Hooker SK, Fahlman A, Moore MJ, Soto NA de, Quiros YB de, Brubakk AO, et al. (2012) Deadly diving? Physiological and behavioural management of decompression stress in diving mammals. Proc R Soc B 279: 1041-1050.

Kvadsheim P, Miller PJO, Tyack PL, Sivle LD, Lam FPA, Fahlman A (2012) Estimated tissue and blood N2 levels and risk of decompression sickness in deep-, intermediate-, and shallow-diving toothed whales during exposure to naval sonar. Frontiers in Physiology 3.

Lawson JW, Stevens TS (2014) Historic and current distribution patterns, and minimum abundance of killer whales (Orcinus orca) in the north-west Atlantic. Journal of the Marine Biological Association of the United Kingdom 94: 1253-1265.

Miller PJO, Shapiro AD, Deecke VB (2010) The diving behaviour of mammal-eating killer whales (Orcinus orca): variations with ecological not physiological factors. Canadian Journal of Zoology 88: 1103-1112.

Moore JE, Merrick RL, Angliss R, Barlow J, Bettridge S, Caretta J, et al. (2011) Guidelines for Assessing Marine Mammal Stocks: Report of the GAMMS III Workshop, February 15-18, 2011, La Jolla, California. US Department of Commerce, National Oceanic and Atmospheric Administration, National Marine Fisheries Service, Office of Protected Resources.

Mullin KD (2007) Abundance of cetaceans in the oceanic Gulf of Mexico based on 2003-2004 ship surveys. 26 pp.

Mullin KD, Fulling GL (2004) Abundance of cetaceans in the oceanic northern Gulf of Mexico. Mar. Mamm. Sci. 20(4): 787-807.

Palka DL (2006) Summer Abundance Estimates of Cetaceans in US North Atlantic Navy Operating Areas. US Dept Commer, Northeast Fish Sci Cent Ref Doc. 06-03: 41 p.

Sivle LD, Kvadsheim PH, Fahlman A, Lam FPA, Tyack PL, Miller PJO (2012) Changes in dive behavior during naval sonar exposure in killer whales, long-finned pilot whales, and sperm whales. Frontiers in Physiology 3.

Waring GT, Josephson E, Maze-Foley K, Rosel PE, eds. (2013) U.S. Atlantic and Gulf of Mexico Marine Mammal Stock Assessments – 2012. NOAA Tech Memo NMFS NE 223; 419 p.